Journal of Cleaner Production 271 (2020) 121941

Contents lists available at ScienceDirect

Journal of Cleaner Production

journal homepage: www.elsevier.com/locate/jclepro

Artificial intelligence-enabled context-aware air quality prediction for smart cities

Daniel Schürholz [a, *], Sylvain Kubler [b], Arkady Zaslavsky [a]

[a] Deakin University, School of Information Technology, Faculty of Science Engineering & Built Environment, Melbourne Burwood Campus, 221 Burwood Highway, Burwood, VIC, 3125, Australia
[b] Université de Lorraine, CNRS, CRAN, F-54000, Nancy, France

ARTICLE INFO

Article history:
Received 8 November 2019
Received in revised form
14 April 2020
Accepted 27 April 2020
Available online 5 June 2020

Handling Editor: Bin Chen

Keywords:
Air quality
Sustainability
Smart city
Context-aware computing
Deep neural networks

ABSTRACT

Metropolitan areas around the world are experiencing a surge in air pollution levels due to different anthropogenic causes, making accurate air quality prediction a critical task for public health. Although many prediction systems have been researched and modelled, many of them have neglected the different effects that air pollution has on each individual citizen. Hence, we present a novel context prediction model that includes context-aware computing concepts to merge an accurate air pollution prediction algorithm (using Long Short-Term Memory Deep Neural Network) with information from both surrounding pollution sources (e.g., bushfire incidents, traffic volumes) and user's health profile. This model is then integrated into a tool called My Air Quality Index (MyAQI), which is further implemented and evaluated in a real-life use case set up in Melbourne Urban Area (Victoria, Australia). Results obtained with MyAQI show both that (i) high precision levels are reached (90–96%) when forecasting air quality situations in four air quality monitoring stations, and (ii) the proposed model is highly adaptable to users' individual health condition effects under the same airborne pollutant levels.

1. Introduction

Air pollution is becoming a major health problem that affects millions of people worldwide. Some reports claim that 4.2 million deaths were attributed to the influence of outdoor air pollution in 2015, China and India being in the front line (Cohen et al., 2017; Yin et al., 2017; United Nations, 2018). Pollutants can even indirectly affect citizens when, for example, they permeate into agricultural food products (Ercilla-Montserrat et al., 2018) or even affecting livelihood and well-being in cities (Wang et al., 2019). Because of all these facts and hazards, urgent actions are required to implement effective mitigation measures (Li and Yi, 2020).

In recent years, monitoring, reasoning and predicting environmental phenomena, specifically air pollution levels, is becoming an increasingly important consideration for public institutions such as governments (e.g., to guarantee citizens that the city environment is healthy) (Holgate, 2017; Australian Government, 2018), companies (e.g., to control greenhouse gas emissions that can be subject to pollution fees) (WBG, 1998) or still for researchers and engineers when producing new fuel sources, that will reduce the hazardous emissions of machinery, for example, reducing Hydrocarbon (HC), Carbon Monoxide (CO) and Nitrogen Monoxide/Dioxide (NOx) smoke in diesel (Dhinesh and Annamalai, 2018). For a long time, researchers have been improving Air Quality (AQ) prediction techniques in order to give citizens and governments more accurate information about how healthy (or unhealthy) the surrounding air is (Becerra et al., 2020; Wang et al., 2020; Dean and Green, 2017). Much of the research effort in AQ is dedicated to data-driven models, where a key task is to try and understand the statistical correlation between the different input parameters (Athira et al., 2018; Wang and Song, 2018; Sun and Sun, 2017; Perez and Gramsch, 2016; Feng et al., 2015) and forecasting AQ levels using machine learning (ML) (Ma et al., 2020), specially Deep Learning Neural Networks (DNN) in the recent years (Zhou et al., 2019; Ma et al., 2019), and even considering sparse or incomplete data (Wu et al., 2018). However, much remains to be done to make AQ systems aware of the user's situation (e.g., location, identity, activity, possible health condition, *etc.*), which falls within the scope of context-aware computing (Perera et al., 2013).

Although a few studies have proposed context-aware AQ

* Corresponding author.
E-mail addresses: dschuerh@mpi-bremen.de (D. Schürholz), s.kubler@univ-lorraine.fr (S. Kubler), arkady.zaslavsky@deakin.edu.au (A. Zaslavsky).

https://doi.org/10.1016/j.jclepro.2020.121941
0959-6526/

monitoring and prediction systems (Catalano and Galatioto, 2017; Chen et al., 2016; Kurt and Oktay, 2010), research gap still exists (Ortiz et al., 2019). Among the major gaps, state-of-the-art AQ models mostly fail in considering pollutant sources specific to given geographical areas (e.g., bushfire incidents traffic volumes), and in providing end-users with a personalised and context-aware recommender system to help them making the best decisions depending on their own health (e.g., best paths or means of commuting) (Shi et al., 2019).

In order to overcome the above research gaps, this paper investigates, designs and evaluates a novel context-aware AQ system – *called "MYAQI" (standing for "*My Air Quality Index*")*. Fig. 1 gives an overall overview of the research methodology used to achieve this goal. First, in section 2, a state-of-the-art literature review of outdoor AQ prediction systems is carried out. Aside from discussing their respective *pros* and *cons*, we seek to identify (i) the most important state-of-the-art variables that influence the AQ system performance, as well as (ii) extra context variables to increase the context-awareness level of traditional AQ systems. As emphasised in Fig. 1, these two sets of variables are used as inputs of the proposed AQ prediction tool, called MyAQI, which aims at predicting spontaneous episodes of high pollutant concentrations, while providing end-users with personalised recommendations (e.g., two persons with different health risk factors will receive different level warnings and can adapt their commute path). While Long Short-Term Memory Neural Network (LSTM) is used for prediction purposes, Context Spaces Theory (CST) (Padovitz et al., 2010) is used for personalised recommendation purposes, as will be thoroughly presented in section 3. In section 4, a real-life use case set up in Melbourne (Australia) is presented with a twofold ambition: (i) showcase the practicability of MyAQI in real-life situations; and (ii) evaluate the performance of MyAQI. Note that all acronyms used in the paper are summarised in Appendix A.

2. Air quality: background & related work

Context prediction can be done on any level of context processing, spanning from low-level context prediction to high-level situation abstraction (Sigg et al., 2012) (i.e., past and present contextual information being linked to future ones (Sigg, 2008)). Any AQ system, and more generally any pervasive system that tries to predict some events based on a contextual model must consider certain characteristics of the real world (e.g., via sensors). Fig. 1 provides an overview of the main building blocks underlying a context-aware AQ system, namely:

1. *Air quality monitoring:* many governments have installed AQ sensor networks across their territories to keep track of air pollutant levels. Sensor networks produce data streams consumed by reasoning systems, based on which AQ indexes (AQI) are usually derived/computed;
2. *Air quality prediction:* ML and artificial intelligence are the most widespread techniques used to estimate – *based on datasets obtained from the monitoring stage* – the possible levels for pollutants in the future;
3. *Context-aware air quality:* some AQ systems include context-aware features to make systems aware of situation-specific events, including user peculiarities or site-specific pollution sources.

Thorough literature reviews regarding the three above building blocks are carried out and presented in sections 2.1, 2.2 and 2.3

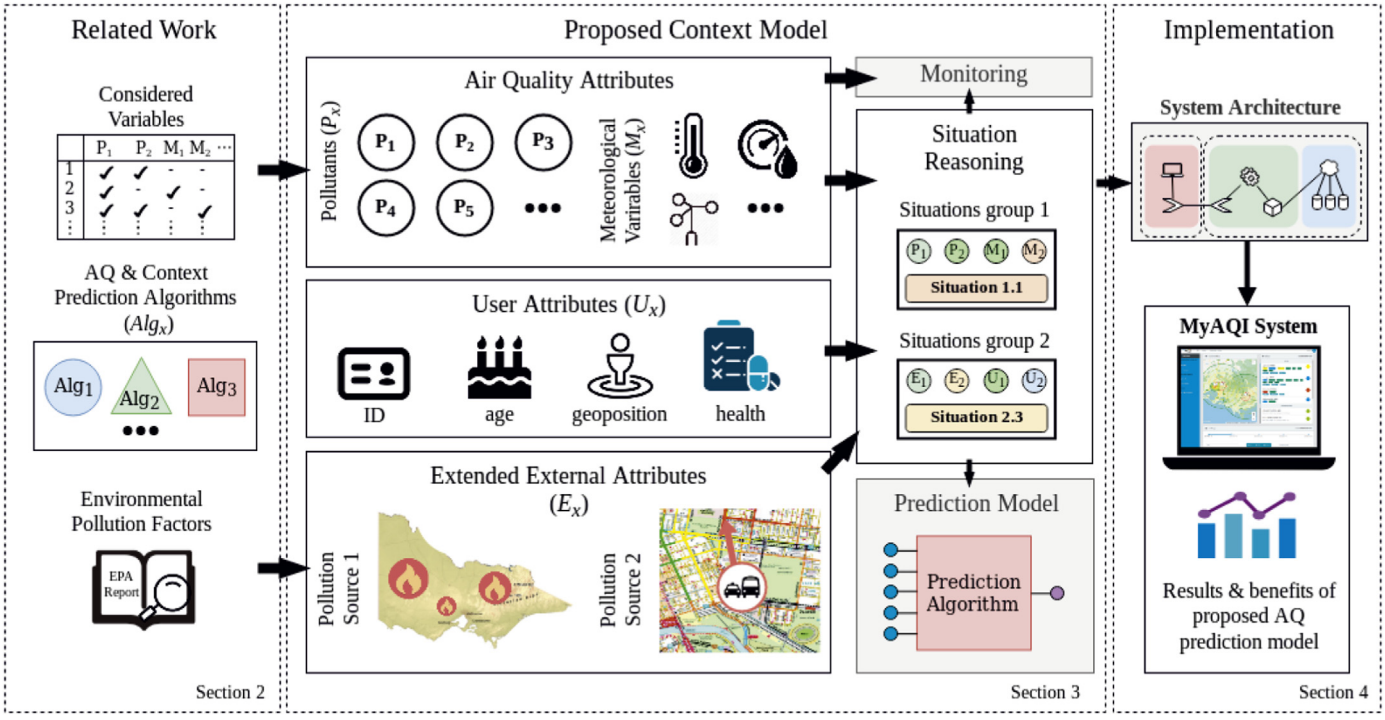

Fig. 1. Research focus, structure and paper layout.

respectively.

2.1. Air quality monitoring

The urge to monitor AQ levels is directly linked to the hazard that airborne pollutants or allergenic agents pose on human health (United States Environmental Protection Agency, 2018). There is big debate about what pollutants are the most hazardous, but most researchers attribute these health hazards to the Particle Matter under 2.5 μm of diameter ($PM_{2.5}$), Particle Matter under 10 μ m of diameter (PM_{10}) and NOx – *Nitrogen Dioxide (NO_2) and Nitrogen Monoxide (NO)* – pollutants. These molecules and particles are all part of what is called chemical air characteristics, a group to which CO, Carbon Dioxide (CO_2), Sulphur Dioxide (SO_2) and Ozone (O_3) belong to. Other outdoor AQ attributes relate to physical phenomena or meteorological data (United States Environmental Protection Agency, 2018), including Relative Humidity (RH), Temperature (T), Wind Speed (WS) and Wind Direction (WD), Luminosity (L), Relative Pressure (RP), Visibility (V), Precipitation (P).

Considering those AQ attributes, we have reviewed and summarised in Table 1 the extent to which each attribute has been considered in AQ -related scientific studies. The most extensively monitored attributes are $PM_{2.5}$, NO and NO_2, even though the others are often considered as they influence on the prediction of these pollutants. Also, meteorological variables are widely measured because of their influence on pollutants concentrations and aerodynamics. The most influential ones are WS, WD, RH and T. Understanding airborne pollution merely from chemical and physical measurements is quite complicated (especially for non-expert users) and thus, a number of Air Quality Indexes (AQI) were introduced all over the world. The ones developed by United States Environmental Protection (US-EPA) (United States Environmental Protection Agency, 2018) and European Environmental Agency (EEA) (Fraser et al., 2016; EEA, 2019, 2020) are today the most widely used. Both indexes are detailed in Appendix B.

2.2. AQ prediction

When referring to AQ prediction or forecast, various approaches can be used to estimate future levels of pollutants. We separate them into five main categories: (i) Fuzzy Logic; (ii) Hidden Markov Models (HMM); (iii) Ensemble models; (iv) Artificial Neural Networks (ANN); and (v) DNN. Sections 2.2.1 to 2.2.5 review research papers that made use of these five respective approaches for AQ purposes.

2.2.1. Fuzzy logic

The first group of prediction techniques uses fuzzy logic, which provides the advantage of non-binary statistical variables. In (Huang and Cheng, 2008), the authors show that AQI can be represented as time series that can significantly change during different annual seasons. They make use of the Ordered Weighted Averaging (OWA) method to aggregate multiple lag periods into single aggregated values by situational weight, outperforming methods such as the simple Moving Average (MA) and Autoregressive Moving Average (ARMA). In (Domańska and Wojtylak, 2012), time series fuzzification is applied to forecast different pollutant concentrations, including PM_{10}, $PM_{2.5}$, SO_2, NO, CO and O_3. Experiments show that their approach outperforms the one proposed by (Huang and Cheng, 2008).

2.2.2. Hidden Markov Models (HMM)

The need for HMM comes from the limitation of simple mapping of problems to states facing regular Markov Models. In (Dong et al., 2009), Hidden Semi Markov Models (HSMM) are used to overcome the state duration problem (i.e., adequate representation of temporal structures for prediction), which consists in clustering the observed values into two categories depending on the value of

Table 1
Air Quality (AQ) attributes used in AQ studies/systems.

	Pollutants						Meteorological Factors						
	$PM_{2.5}$	PM_{10}	NO_x	SO_2	CO	O_3	WIND	RH	T	RP	P	V	L
(Shaban et al., 2016)	–	–	✓	✓	–	✓	–	–	–	–	–	–	–
(Zhao et al., 2010)	–	✓	✓	✓	–	–	✓	✓	✓	✓	✓	✓	✓
(Bai et al., 2016)	–	✓	✓	✓	–	–	✓	✓	✓	✓	✓	✓	✓
(Huang and Cheng, 2008)	–	–	–	–	–	✓	–	–	–	–	–	–	–
(Singh et al., 2012)	✓	✓	✓	✓	–	–	–	–	–	–	–	–	–
(Chen et al., 2016)	✓	✓	✓	–	–	–	–	–	–	–	–	–	–
(Donnelly et al., 2015)	–	–	✓	–	–	–	✓	✓	–	✓	–	–	✓
(Biancofiore et al., 2017)	✓	✓	–	–	✓	–	✓	✓	✓	✓	✓	✓	✓
(Feng et al., 2015)	✓	–	–	–	–	–	✓	✓	✓	✓	✓	–	–
(Sun et al., 2013)	✓	–	✓	✓	✓	–	✓	✓	✓	–	–	–	–
(Dong et al., 2009)	✓	–	–	–	–	–	✓	✓	✓	✓	✓	✓	✓
(Domańska and Wojtylak, 2012)	✓	✓	✓	✓	✓	–	✓	✓	✓	✓	–	✓	–
(Sun and Sun, 2017)	✓	✓	✓	✓	✓	✓	–	–	✓	–	–	–	–
(Perez and Gramsch, 2016)	✓	✓	–	–	–	–	✓	✓	✓	–	–	–	–
(Catalano and Galatioto, 2017)	–	–	✓	–	✓	–	–	–	–	–	–	–	–
(Wang and Song, 2018)	✓	✓	✓	✓	✓	✓	✓	✓	✓	–	–	–	–
(Athira et al., 2018)	–	✓	–	–	–	–	✓	✓	✓	–	✓	✓	–
(Qi et al., 2019)	✓	✓	✓	✓	✓	✓	✓	✓	✓	✓	–	–	–
(Zhu et al., 2018)	✓	–	–	–	–	–	✓	✓	✓	✓	–	–	✓
(Zhou et al., 2019)	✓	✓	✓	✓	✓	✓	✓	✓	✓	–	✓	–	–
(Wen et al., 2019)	✓	–	–	–	–	–	✓	✓	✓	–	–	–	–
(Li et al., 2017)	✓	–	–	–	–	–	✓	✓	✓	–	–	✓	–
(Ong et al., 2016)	✓	–	–	–	–	–	✓	✓	✓	–	✓	–	✓
(Huang and Kuo, 2018)	✓	–	–	–	–	–	✓	–	–	–	✓	–	–
(Kurt and Oktay, 2010)	–	✓	–	✓	✓	–	✓	✓	✓	✓	–	–	–
	17	13	13	11	9	6	19	18	18	10	9	7	7

Table 2
Criteria taxonomy used to classify in Table 3 the scientific articles reviewed throughout Section 2.

Taxonomy criteria *(numbering used in Table 2)*		Framework
Reference	(a) Approach	Research work for the proposed method.
Algorithm	(b) Type	Category of the algorithm (ANN, SVM, Linear Regressor, HMM…).
	(c) Method	The method used in the research work (Fuzzy sets, RNN…).
Parameters	(d) AQ Input Variables	CO, CO_2, NO_2, O_3, PM, $PM_{2.5}$, PM_{10}, SO_2, Not Specified(N/S)
	(e) Meteorological Input Variables	Precipitation (P), Relative Humidity (RH), Relative Pressure (RP), Temperature (T), Visibility (V), Wind Direction (WD), Wind Speed (WS)
	(f) Feature Extraction	If and name of the preprocessing algorithm used to extract features.
	(g) Extended Context	If and names of the extra non-AQ attributes considered.
Performance	(h) Statistical Performance Indicators	Indicators used in this specific work (e.g., RMSE, PA…).
	(i) Comparison References	If and what algorithms is used for comparison benchmark purposes.
	(j) Output Variables	What AQ attributes are used as an output of the proposed algorithm.
Dataset	(k) Definition	Geographic location from where the data was retrieved.
	(l) Other Characteristics	Number of stations (sta.) and/or records for training and test sets (rec.).

highest log-likelihood. In (Sun et al., 2013), a more extensive approach is presented, consisting in applying a HMM with non-Gaussian distributions and Wavelet Decomposition (WavD), which has been proven to improve the True Prediction Rate (TPR) and reduce false alarms.

2.2.3. Ensemble models

Other methods integrate a mix of techniques like the LS-SVM with Principal Component Analysis (PCA) and Cuckoo's Search Algorithm (CSA) presented in (Sun and Sun, 2017), where CSA is applied to improve the regular Support Vector Machines (SVM) selection process of parameters, that suffers from speed and convergence accuracy issues. Another approach combining two distinct modelling techniques (parametric and non-parametric) is proposed in (Donnelly et al., 2015) to provide real-time hourly forecasts of NO_2. Experiments show that the combination of these two techniques leads to more accurate daily forecasts than when applied individually.

2.2.4. Artificial Neural Networks (ANN)

ANN and deep learning are some of the fastest and most dynamic developing areas in AI. Various studies (Singh et al., 2012; Shaban et al., 2016) reveal that data used for AQ prediction is generally non-linear, thus requiring specific techniques to tackle it. ANNs are one of such techniques. Singh et al. (Shaban et al., 2016) propose and compare three distinct techniques to predict O_3, SO_2 and NO_2, namely: (i) regular SVM; (ii) Simple Perceptron ANN; and (iii) Multivariate Regression Tree (MP5). Results show that MP5 provides more accurate results but turns out to be complex to implement. In (Singh et al., 2012), an approach using Partial Least Squares Regression (PLSR) and Multivariate Polynomial Regression (MPR) is proposed, which is proven to outperform the Multi-Layer Perceptron (MLP), Radial-Basis Function Neural Network (RBFNN) and Generalized Regression Neural Network (GRNN) techniques. In (Biancofiore et al., 2017), a comparison of the Recurrent Neural Network (RNN), non-recursive Back-Propagation Neural Network (BPNN) and MPR techniques for $PM_{2.5}$ concentration prediction is carried out, whose results show that the ANN with recursive structure performs better than MPR this finding is confirmed in (Feng et al., 2015)).

An interesting yet important observation made by the previous studies is that, the higher the number of low-frequency high pollutant concentration peaks, the harder it is to achieve good predictions with ANN tecniques. Another key lies in how to select the right parameters for the prediction algorithm. In this respect, a ga-based approach combined with a rbfnn is proposed in (Zhao et al., 2010), while in (Bai et al., 2016) bpnn and wd are combined for parameter tuning.

2.2.5. Deep neural networks (DNN)

In recent years, the focus of ML techniques has hugely shifted towards DNN algorithms because of their accuracy for solving previously unattainable problems, and this goes far beyond the AQ domain.

In the AQ literature, Long Short-Term Memory Neural Network (LSTM) is the most widely applied DNN techniques, even though other DNN techniques have been applied, as in (Ong et al., 2016; Zhu et al., 2018). Looking at studies using LSTM, Wang et al. (Wang and Song, 2018) propose a two-step approach that consists, first, in summarising the temporal properties of AQ into two short-term and long-term dependencies, and then in learning both thanks to LSTM. In (Athira et al., 2018), the authors explain that the time changeability of AQ prediction is 10 or more days, which is longer than the one of climate estimates (4–5 days usually) and therefore present a comparison of three DNN techniques: RNN, LSTM and Gated Recurrent Unit (GRU). GRU seems to better fit the AQ prediction problem because it models the intricate relations of AQ changeability and meteorological factors. In (Qi et al., 2019), Graph Convolutional Network (GCN) and LSTM are combined to predict the mass concentration of $PM_{2.5}$ at a desirable time, the former technique being applied to extract the spatial dependency between different meteorological monitoring stations, and the latter for capturing any temporal dependency (e.g., between air pollutants and meteorological data). In (Li et al., 2017), an extended LSTM is proposed to capture dependencies of air pollutant concentrations from a long-term spatio-temporal perspective, including, among other dependencies, seasonality, months or still time-of-day. In (Zhou et al., 2019), a DNN-based multi-output LSTM model is presented, whose results show that the achieved accuracy clearly outperforms other versions of the LSTM network. A final approach using LSTM is presented in (Huang and Kuo, 2018), in which a combination of Deep Convolutional Networks (CNN) and LSTM is developed to predict $PM_{2.5}$ at the city level. This approach also outperforms traditional techniques such as Random Forest, Decision Tree, MLP and the Simple LSTM.

2.3. Towards context-aware air quality solutions

As stated by EEA, the age and health conditions – *especially cardiovascular and respiratory* – significantly influence people's vulnerability towards airborne pollutants (EEA, 2019). Among

Table 3
Classification of the scientific articles reviewed throughout Section 2 (the columns' meaning is described in Table 2.

(a)	(b)	(c)	(d)	(e)	(f)	(g)	(h)	(i)	(j)	(k)	(l)
(Huang and Cheng, 2008)	Fuzzy Logic	OWA	O_3	–	–	–	RMSE,MAD, MAPE, MSE	MA, ARMA	O_3	Hsinchu [Jul 2004–Aug 2007]	1061 rec.
(Zhao et al., 2010)	ANN	RBFNN	SO_2, NO_2, PM_{10}	T, RH, WS, WD, P, V, L, RP	GA	–	ARE, R	RBFNN, PCA-ANN	SO_2, NO_2	Tianjing [2003 –2007]	–
(Dong et al., 2009)	Markov Model	HSMM - Gaussian PDF	$PM_{2.5}$	T, RH, WS, WD, CL, DP, SR, RP	–	–	Log-likelihood	Ground-truth	$PM_{2.5}$	Chicago [2000 –2001]	12 sta.
(Kurt and Oktay, 2010)	ANN	GFM-NN	SO_2, CO, PM_{10}	T, RH, WS, WD, RP	–	Locations	Band error	Other geo models	SO_2, CO, PM_{10}	Istanbul [Aug 2005 to Jul 2006]	10 sta.
(Singh et al., 2012)	ANN	GRNN	SO_2, NO_2, PM_{10}, $PM_{2.5}$	–	–	–	RMSE, MAE, Ef, Af, R, SEP	PLSR, MPR, MLP, RBFNN	SO_2, NO_2,PM^{10}, $PM^{2.5}$	Lucknow [Jan 2005–Dec 2009]	5 sta.
(Domańska and Wojtylak, 2012)	Fuzzy Logic	Fuzzy Sets	SO_2, NO_2, CO, PM_{10}, $PM_{2.5}$	T, RH, WS, WD, RP, V	–	–	Undefined error rate	Ground truth	SO_2, NO_2, CO, PM_{10}, $PM_{2.5}$	Poland [2002 –2009]	15 sta.
(Sun et al., 2013)	Markov Model	hmm	SO_2, NO_2, CO, $PM_{2.5}$	T, RH, WS, WD	WavD	–	TPR, FAR, SI, K–S	HMM - normal PDFs	$PM_{2.5}$	California [1999 –2011]	2 sta.
(Donnelly et al., 2015)	Other	Param. & non-Parametric	NO_2	RH, WS, WD, L, RP	–	–	R, IA, FB, FAC_2	Ground truth	NO_2	Dublin [2007 –2012]	4 sta.
(Feng et al., 2015)	ANN	BPNN - LM	$PM_{2.5}$	T, RH, WS, WD, P, RP	WavD	GT	RMSE, MAE, IA, DR, FAR	bpnn, bpnn + gt	$PM_{2.5}$	Beijing [2013 –2014]	4 sta.
(Shaban et al., 2016)	Other	M5P Tree	SO_2, NO_2, O_3	–	–	–	RMSE, PTA	ANN, SVM	SO_2, NO_2, O_3	Qatar [June to August 2013]	1 sta.
(Bai et al., 2016)	ANN	BPNN	SO_2, NO_2, PM_{10}	T, RH, WS, WD, P, V, L, RP	WavD	–	RMSE, MAPE, R	BPNN	SO_2, NO_2, PM_{10}	Chongqing [1 year]	360 rec.
(Chen et al., 2016)	Other	Semi-super. & Pruning	NO_2, PM_{10}, $PM_{2.5}$	–	–	Traffic, Road, PoI, Check-in	RMSE, Af	GPR, U-Air, U-Air(-Fc), U-Air(+kNN)	NO_2, PM_{10}, $PM_{2.5}$	Huangzhou [Nov 2013–Sep 2014]	6 sta.
(Perez and Gramsch, 2016)	ANN	MLP-BP	PM_{10}, $PM_{2.5}$	T, RH, WS, WD	Input Prunning	Thermal	R, NPEt, PEt	MLR	$PM_{2.5}$	Santiago [2010 –2012]	2 sta.
(Ong et al., 2016)	DNN	RNN - DynPT	$PM_{2.5}$	T, RH, WS, WD, P, L	–	–	RMSE, Prec., Recall, F1-sco.	VENUS-Japan, rbm, arima, mlp	$PM_{2.5}$	Japan [2 years]	52 sta.
(Biancofiore et al., 2017)	ANN	RNN	CO, PM_{10}, $PM_{2.5}$	T, RH, WS, WD, P, V, L, RP	–	–	NMSE, FB, FAC2, R	MLR, ANN	$PM_{2.5}$	Pescara [2011 –2013]	1 sta.
(Sun and Sun, 2017)	svm	ls-svm	SO_2, NO_2, O_3, CO, PM_{10}, $PM_{2.5}$	T	CSA, PCA	–	RMSE, MAE, MAPE	LS-SVM, GRNN	$PM_{2.5}$	Henbei [2015]	–
(Catalano and Galatioto, 2017)	Other	ARIMA, SARIMA	NO_2, CO	–	–	Site model	R, MAPE	MLP	NO_2	Bury & London [2010]	2 sta.
(Li et al., 2017)	DNN	LSTM	$PM_{2.5}$	T, RH, WS, WD, V	–	Stationary timestamp	RMSE, MAE, MAPE STDL	STDL, TLNN, LSTM, ARMA, SVR	$PM_{2.5}$	China [Jan 2014 –May 2016]	12 sta.
(Wang and Song, 2018)	DNN	LSTM	SO_2, NO_2, O_3, CO, PM_{10}, $PM_{2.5}$	RMSE, MAE, MAPE	Grang., FC-M	Spatio-temp.	RMSE, MAE, PA LR	lr, rt, ae, ffa	$PM_{2.5}$	Beijing [2013 –2017]	35 sta.
(Athira et al., 2018)	DNN	RNN, LSTM, GRU	PM_{10}	T, RH, WS, WD, P, V	–	Spatio-temp.	RMSE, MAE, MAPE	Simple rnn	PM_{10}	China [Apr 2015 –Sep 2017]	1498 sta.
(Zhu et al., 2018)	DNN	GRNN	$PM_{2.5}$	T, RH, WS, WD, L, RP	CEEMD, PSOGSA, SVR,GCA CNN	Spatio-temp.	RMSE, MAE, MAPE, IA, R	CEEMD, EEMD mixes, PSOGSA-SVR, AE, FFA	PM2.5	China [Dec 2013 –Aug 2015]	–
(Huang and Kuo, 2018)	DNN	LSTM	PM2.5	WS, WD, P	CNN	Spatio-temp.	RMSE, MAE, IA, R	SVM, RF, DT, MLP, CNN, LSTM	$PM_{2.5}$	Beijing [2010 to 2014]	–
(Qi et al., 2019)	DNN	LSTM	SO_2, NO_2, O_3, CO, PM_{10}, $PM_{2.5}$	SO_2, NO_2, O_3, CO, PM_{10}, $PM_{2.5}$	Graph-cnn	Spatial correlation	RMSE, MAE, IA, RR, FAR	MLR, FF-ANN, LSTM	$PM_{2.5}$	Jing-Jin-Ji [Jan 2015–Apr 2016]	76 sta.
(Zhou et al., 2019)	DNN	DM-LSTM	SO_2, NO_2, O_3, CO, PM_{10}, $PM_{2.5}$	SO_2, NO_2, O_3, CO, PM_{10}, $PM_{2.5}$	–	Spatio-temp.	RMSE, Gbench	SM-LSTM, DMLSTM(1-3)	NO_2, PM_{10}, $PM_{2.5}$	Taipei [2010 –2016]	21 sta.
(Wen et al., 2019)	DNN	C-LSTME	$PM_{2.5}$	T, WS, Planet. Bound heig., Aero. depth, RH	Station cluster.	Spatio-temp. correlation	RMSE, MAE, MAPE	LSTM, STDL, LSTM, Zheng, ARMA, SVR, LR	$PM_{2.5}$	China [Jan 2016 –Dec 2017]	12 sta.

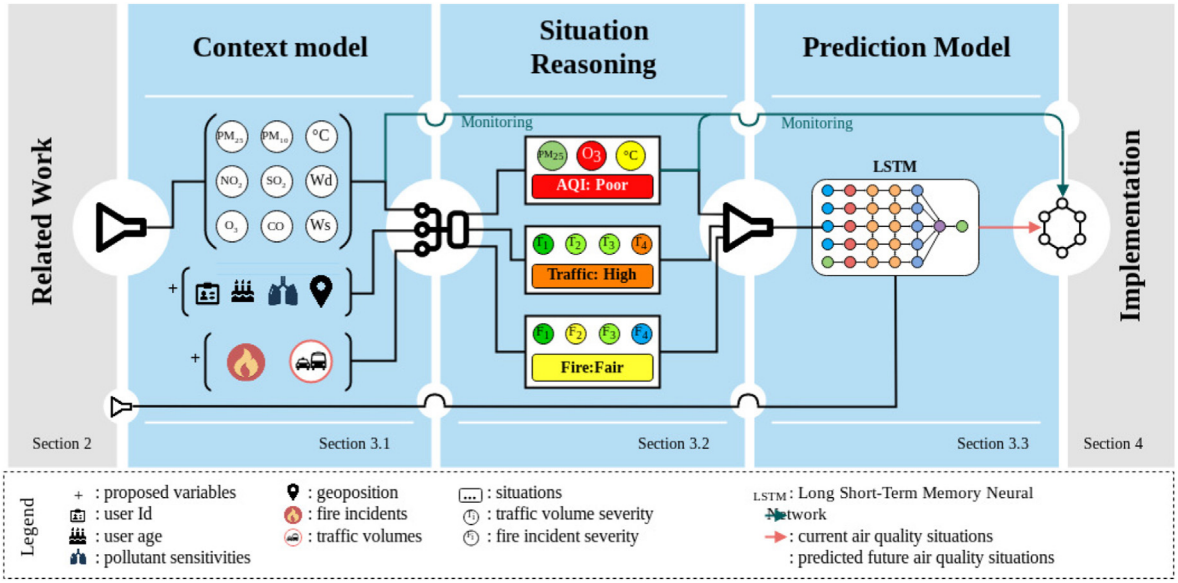

Fig. 2. Building blocks of the proposed context-aware AQ prediction system (MyAQI).

other reports, the technical assistance document released by US-EPA (United States Environmental Protection Agency, 2018) provides a relevant overview of the hazards for people with certain health conditions. All this to say that personalised information (e.g., users' health conditions) must be taken into account, whenever possible, when computing or concluding about the criticality of any AQ level. The motivation beyond this paper and proposing a novel context-aware AQ system lies in the fact that the current AQ literature fails to properly cover the context-aware dimension. To support this statement, we propose in Table 3 a synthesis of what AQ features/criteria are supported by state-of-the-art models/tools. Columns (a) to (l) in Table 3 refers to the set of features/criteria referenced in Table 2, which has been structured based on what has been discussed trough sections 2.1 and 2.2. Even though the following mainly discusses of the context-awareness dimension i.e., column (g)), we believe that Table 3 provides readers with a very comprehensive view of the current state-of-the-art on AQ.

Looking more specifically at column (g), we can see that most of the reviewed papers do not consider any external context attribute (i.e., for pollution sources or user's health indicators), or in a very limited fashion (e.g., ONLY considering the geographical relationship between monitoring station). Only (Chen et al., 2016) considers many contextual attributes, although neglects the pollutant level measurements. In (Dutta et al., 2009) a personal and portable AQ monitoring system is introduced that tells the users, in real-time, the surrounding air conditions based on the US-EPA AQI. Although the real-life test case (involving 16 participants) is convincing, the proposed system does not include any prediction capability. Other studies did consider air pollution forecasting solutions along with context-aware features. (Kurt and Oktay, 2010), for example, presents an ANN-based approach that integrates a geographic relationship model for sensor stations. More recently, Wen et al. (2019) published a convolutional LSTM neural network model that integrates auxiliary data, including meteorological and aerosol optical depth data. Overall, the auxiliary data helps to reach more accurate predictions under highly changing AQ conditions. In (Catalano and Galatioto, 2017), the authors explain that pollution situations should be treated as individual cases depending on the user's location and context. Accordingly, the authors develop a self-managing model to select, for each specific combination of pollution emission and dispersion factors, the most suitable prediction model within a set of alternative AQ models. Their proposal is tested on two distinct sites in the UK, which has evidenced an impressive gain compared to only using a general approach (up to 113%). In our opinion, this approach is very promising, although it can still be improved considering more efficient prediction techniques (*cf.*, section 2.2). Finally, an approach expanding the common set of context attributes used in most of the prediction algorithms is designed in (Chen et al., 2016), which consists in, first, dividing the monitored region into a grid of equally sized squares, and then in considering a set of different attributes inside each square.

Overall, all the above-introduced studies are encouraging efforts towards context-driven AQ solutions. Having said that, there is still research to be done to overcome some limitations, namely:

- The vast majority of the works we researched focus on improving the underlying machine learning algorithms, fine-tuning parameters and applying new techniques.
- Other proposals rely completely on only external data to the problem of predicting AQ.
- No study, to the best of our knowledge, has proposed to combine both approaches despite of the benefits that could be derived;
- There is also limited research towards including pollution sources into the AQ prediction models.
- No other study considers the use of context-aware computing to provide a framework to combine the AQ prediction using time-series of pollutants and meteorological factors, with other contextual information such as pollution sources.
- Proposed solutions in the literature rarely try to improve on the way that information is conveyed to the stakeholders, for a better understanding.

Our research seeks to overcome the above limitations with the design of a novel context-aware AQ prediction system, which is the presented in Section 3.

Table 4
Set of MyAQI system *Context Attributes* with their format, value ranges, units of measurement and examples.

- *Extended external attributes:* extra air pollutant data sources considered as part of our modelling are: (i) *Traffic volume:* considered as one of the primary sources of pollution in cities and contribute largely to high NO_2 and CO levels (EEA, 2019; EPA Victoria, 2013); (ii) *Fire incidents:* they largely contribute to the pollution ($PM_{2.5}$, PM_{10}) in urban areas surrounded by dry vegetation areas (EPA Victoria, 2013);
- *User attributes:* the following user attributes are considered: (i) *User Id:* identifies a user for a customised experience; (ii) *Geo-location:* determines the spatial reference of a user's location; (iii) *Timestamps:* specific time and date of interaction; (iv) *Pollutant sensitivity:* represents the level of influence that a given pollutant has on the user using a 6-pollutant sensitivity level scale, which is derived from a small questionnaire at the system's profile section, as presented in (Nurgazy et al., 2019).

	Attribute	Format	Range	Unit	Example
AQ	$PM_{2.5}$	decimal	$[0, +\infty[$	$\mu g/m^3$	4.5
	PM_{10}	decimal	$[0, +\infty[$	$\mu g/m^3$	30.25
	NO_2	decimal	$[0, +\infty[$	ppb	40.74
	O_3	decimal	$[0, +\infty[$	ppm	55.11
	SO_2	decimal	$[0, +\infty[$	ppb	24.9
	CO	decimal	$[0, +\infty[$	ppm	328.0
	AQI	integer	$[0, +\infty[$	–	62
Meteo	T	decimal	$[-\infty, +\infty[$	°C	18.0
	RH	decimal	$[0, 100]$	%	77.87
	WS	decimal	$[0, +\infty[$	*m/s*	2.3
	WD	decimal	$[0, 360]$	degrees	235.5
Extended	Traffic	integer	$[0, 4]$	traffic volume	4
	Fire Incident	integer	$[0, 5]$	distance to user	2
User	User Id	String	Alpha-numeric	–	alice
	Age	integer	$[0, 200]$	years	66
	Geo-Location	decimal	$lat \in [-90, 90]$ $lon \in [-180, 180]$	degrees	lat: −34.42, lon: 140.64
	Pollutant Sensitivity	integer	$[0, 4]$	sensitivity level	co: 0, o3: 2, …

3. MyAQI: context-aware AQ prediction system

The proposed context-aware AQ prediction system, called "My Air Quality Index" (MyAQI), consists of three building blocks as depicted in Fig. 2, namely: (i) Context modelling, (ii) Situation reasoning; and (iii) Prediction model. The theoretical and architectural design choices made for each building block are respectively detailed in sections 3.1, 3.2 and 3.3.

3.1. Context modelling

As any context-aware approach, the first step consists in the modelling phase (Perera et al., 2013). The Context Space Theory (CST) formalised in (Padovitz et al., 2010) is used in this respect, as it has proven to be a robust and simple tool to formalise real-life phenomena to a computational model. According to this theory, first the *application space* must be defined, which encompasses all of the variables and values comprising the model. *Context spaces* are subsets of this space, formalised as *N*-dimensional Euclidean spaces defined over a collection of *context attributes*, where *N* represents the number of attributes selected. A *context attribute* represents a specific feature, critical to fulfil the system's functions. Each attribute consists of an Id, a value type and a range of values that it can get assigned within the *context space*. *Context states* are the collections of values assigned to each *context attribute* during the system functioning. Finally, a *Situation* represents an event in the real world and belongs to one or more *situation spaces*, which are a subset of the *context space*. In CST, situations can be derived as the result of intersecting *Context States* to *Situation Spaces*. For example, in the Melbourne use case (presented in Section 4), the application space is comprised by the different pollutants and meteorological factors as its main context attributes, where their values change over time, forming a time-series (each step in the time-series being a context state). Situations in this scenario are represented by AQ categories, like "very poor" air quality; and a situation is known to be happening if the context state values fall within the value ranges of the context attributes that are specified for it.

Table 5
Situation space definition for AQ-related attributes.

AQI categories	User Sensitivity Levels				
	0	1	2	3	4
Very Good	0–33	0–33	0–33	0–33	0–23
Good	34–66	34–66	34–66	34–54	24–44
Moderate	67–99	67–99	55–79	55–79	45–59
Poor	100 - 149	100 - 124	80–89	80–89	60–69
Very Poor	≥150	≥125	≥ ≥100	90	≥70

Given the above definitions, context attributes and situations that are relevant for My Air Quality Index (MyAQI) should be specified. Four categories of context attributes are specified, which are separated into four categories as given in Table 4:

- *AQ attributes:* based on the findings from our literature review (see Section 2.1), the following attributes are selected as part of our modelling: (i) *$PM_{2.5}$:* related to deaths caused by air pollution (often caused by dust concentrations or smoke from open fires); (ii) *NO_2:* gas produced by the burning of fossil fuels (highly dangerous); (iii) *PM_{10}, SO_2, CO*: directly related to $PM_{2.5}$ and NO_2 concentrations; (iv) *O3:* related to other pollutants in warm temperatures (dangerous in high concentrations); (vi) *AQI:* it corresponds to a *context-derived attribute* and it does not originate directly from sensor equipment but is calculated from the pollutants' atomic measurements
- *Meteorological attributes:* they are crucial to understand the behaviour of "already emitted" pollutants, as they affect their location, distribution and temporality. The following attributes are considered: (i) *T:* it affects the characteristics of gases by making more or less airborne (Kalisa et al., 2018); (ii) *RH*: lower humidity enables pollutant particles to become more airborne (Qiu et al., 2013); (iii-iv) *WS and WD*: related to the dynamics of air pollutants.

3.2. Situation Reasoning

Following the CST approach, *situation spaces* must then be specified. Three situations are specified in MyAQI, as described in the following.

Situation 1: it refers to the AQI, which is based in our study on the auepa[1] due to the targeted use case (setup in Melbourne). This index is formalised in Eq. (1), which has been defined in (United States Environmental Protection Agency, 2018), with I_p the index for pollutant p; C_p the truncated concentration of pollutant p; BP_{Hi}

[1] The situation space specification considering the US-EPA and EEA indexes is available in Appendix C.

Table 6
Situation space definition for traffic-related attributes.

Traffic volume	Situation Id	Quantile	Value Range
Very low	0	Q_1(0%–20%)	$[0, q_1]$
Low	1	Q_2(20%–40%)	$]q_1, q_2]$
Moderate	2	Q_3(40%–60%)	$]q_2, q_3]$
High	3	Q_4(60%–80%)	$]q_3, q_4]$
Extremely High	4	Q_5(80%–100%)	$]q_4, +\infty[$

Table 7
Situation space definition for fire-related attributes.

Fire severity	Situation Id	City range (kms)	Suburban range (kms)
No fire	0	$]20, +\infty[$	$]100, +\infty[$
Very low	1	$[16, 20]$	$[80, 100]$
Low	2	$[12, 16[$	$[60, 80[$
Moderate	3	$[8, 12[$	$[40, 60[$
High	4	$[4, 8[$	$[20, 40[$
Extremely High	5	$[0, 4[$	$[0, 20[$

the concentration breakpoint (which is $\geq C_p$); BP_{Lo} the concentration breakpoint (which is $\leq C_p$); I_{Hi} the AQI value corresponding to BP_{Hi}; and I_{Lo} the AQI value corresponding to BP_{Lo}. This index then serves as an objective indicator of air quality regarding human health conditions, to which pollutant sensitivities are mapped, as given in Table 5. A sensitivity score of 0 means that the a user is influenced negatively only if the level of air pollution is extremely high and thus dangerous for any person no matter the health condition, while 4 means the user will likely suffer negative effects rather quickly (usually caused by a pre-existing respiratory health condition, such as asthma), even with lower levels of air pollution.

$$I_p = \frac{I_{Hi} - I_{Lo}}{BP_{Hi} - BP_{Lo}} - (C_p - BP_{Lo} + I_{Lo}) \quad (1)$$

Situation 2: it refers to the traffic volumes, which are relative to the road type and the traffic volume measuring stations (usually deployed on road crossings) where data was collected. Hence, percentages are used for defining the severity of a given measurement, where values are calculated from five quantiles for each traffic station's traffic volume's data. Quantiles are the Q groups obtained from dividing the range of a probability distribution into (nearly) equal sized parts, divided by $Q-1$ values of the form: $0 < q_i \leq Q-1$. Five quantiles are considered as a fair representation of possible traffic situations, as specified in Table 6, spanning from "very low' (0)' to "extremely high (4)".

Situation 3: it refers to fire incidents, which are categorised according to the distance to the AQ measuring stations (the closer the incident to the station, the higher the severity). They are divided into urban and suburban (and/or countryside) scenarios because of the size of incidents in each case as well as possible obstacles that could stop the spread of smoke/ashes. For stations in cities, we arbitrarily propose to consider a distance of 20*kms* to be relevant and for those in the outskirts of the urban area or countryside, a distance of 100*kms*; then the other distances are five equals fraction of these distances, as specified in Table 7.

The outcome of the reasoning stage and deducted situations are used as inputs of the prediction model, which is detailed in the next section.

Algorithm 1. PredictAQSituation(U, S, AQI, dP)

input : U, S, AQI, dP; // The active user (U), the selected AQ measuring station (S), the AQI type (e.g., AUEPA AQI) (AQI) and the desired pollutant to be predicted (dP)
output: AQS_p; // The predicted AQ situation considering the user's health condition

begin
  $C_{aq} \longleftarrow getAQAttrsForStation(S)$; // Retrieving AQ context attributes for station S
  $C_{ex} \longleftarrow getExtendedAttrsForStation(S)$; // Retrieving extended context attributes for station S
  $C_{us} \longleftarrow getHealthCondAttrsForUser(U)$; // Retrieving health condition context attributes for user U
  $T \longleftarrow \{aq_1 : [], \ldots, aq_n : [], ex_1 : [], \ldots, ex_m : []\}$; // The initialised time series, with lists of values for AQ and extended context attributes
  for $t \leftarrow getStartTime(24)$ **to** $getCurrentTime()$ **by** 1 **do** // Retrieve data since 24 hours ago in one hour increments
    for $ex_i \in C_{ex}$ **do** // Get each extended context attribute
      $T[ex_i] \longleftarrow getExtAttrSituation(ex_i, S, t)$; // Retrieve the situation for extended context attribute ex_i regarding station S at time t and add to time series.
    for $aq_i \in C_{aq}$ **do** // Get each AQ attribute
      $T[aq_i] \longleftarrow getAQContextAttrState(aq_i, S, t)$; // Retrieve the context state for AQ attribute aq_i regarding station S at time t and add to time series.
  $T_n \longleftarrow prepareForPrediction(T)$; // Normalising and formatting the time series to feed data into the prediction algorithm
  $PC_p \longleftarrow LSTMprediction(T_n, dP)$; // Predict the concentration for the next hour for the desired pollutant, using the pre-trained LSTM DNN model
  $AQS_p \longleftarrow getAQCategory(P_p, C_{us}, AQI)$; // Transform the predicted pollutant concentration (PC_p) in to an Air Quality Situation (AQS_p)
  return AQS_p; // The predicted AQ situation is what we will show to the user

3.3. Prediction

Including a prediction model that consumes the environmental AQ and extended context attributes to predict situations requires to adopt a reliable prediction technique. Our literature review (*cf.*, Section 2), has shown that ANN and DNN techniques are the most widely used for AQ prediction purposes. However, one downside of these techniques is that they fall into a category known as black-box methods, which makes it challenging to understand the underlying process. HMM techniques, on the other hand, can give more insight on the statistics obtained, but the accuracy that current DNN offer, especially LSTM, surpasses their deficiencies. Given the nature of AQ datasets (time-series) and the promising results obtained with DNNs in the literature (DNNs outperforming almost all the older data-based regression models), we adopt a LSTM DNN approach/model in this research work.

A LSTM DNN, first introduced in (Hochreiter and Schmidhuber, 1997), is a type of gated RNN that keeps information for long time dependencies (dependencies that were neglected by former ANN models). It consists of an input layer that takes the incoming features, followed by one or more recurrently interconnected hidden layers, also know as memory blocks, and an output layer that produces the final regression result. A more detailed explanation of the LSTM theory is provided in Appendix D. The LSTM DNN structure adapted to MyAQI is illustrated in Fig. 3. It takes as inputs the time series for AQ, meteorological and extended context variables, the latter variable (extended) being transformed through the *Situation Reasoning* model to the values relevant to each situation. All the variables – *AQ, meteorological and extended ones* – are then normalised to values between 0 and 1, further feeding the LSTM DNN layer. The DNN depends on some hyper-parameters such as batch size, hidden layers numbers, neurons numbers per layer, *etc.*, which have to be twitched and tested to achieve an heuristically best outcome. With these parameters, the LSTM's training epochs are executed, the error loss calculated, and a validation set used to guarantee the model fitness. The outcome of the LSTM DNN layer is forwarded to a fully-connected ANN (FCNN), whose outcome is the predicted value set for the desired pollutant for different time lags (i.e. $P_{1(t+1)} \dots P_{1(t+24)}$). Lastly, the pollutant predictions are used to reason the AQ situation at the given point in time.

The model shown in Fig. 3 can be better understood by referring to Algorithm 1, which presents the process to predict an AQ situation AQS_p for a desired pollutant *dP*, an active user *U*, a selected AQ monitoring station *S* and a selected *AQI* index scale (e.g., the AU-EPA AQI). First the algorithm retrieves all relevant AQ context attributes C_{aq} and extended context attributes C_{ex} according to the selected station *S*. The selection of these attributes depend on their availability on the monitoring station, the correlation between AQ attributes to the prediction of *dP* and the probable impact of extended attributes around the area where *S* is located. The next step is to get the user context attributes C_{us} regarding *U* (e.g., pollutant sensitivity levels) in order to customise the output of the algorithm. Then the algorithm builds an empty dictionary *T* with each AQ and extended attribute as keys, each having an empty list assigned. Next, it iterates over the last 24 h in 1-h time steps and selects the context state (value) for each AQ attribute aq_i and extended attribute ex_i. The transformation of the extended attributes follows the situation tables presented in Section 3.2. Each value is added to its corresponding list in the time-series *T*, which is then normalised and formatted generating T_n. T_n is fed into the LSTM DNN prediction model, which was pre-trained using historical data, in the same type of time increments. The prediction function takes *T* and *dP* as inputs and provides the prediction of *dP*'s concentration for the next hour PC_p. This value is then transformed into a AQ situation AQS_p, which considers the health conditions of the user, using the pollutant sensitivity levels. The AQS_p value can be used to present information to the user or trigger notifications.

3.4. Context-aware air quality system architecture

All the previously introduced steps(situation modelling, prediction models) have been implemented into a software program, whose architecture consists of three layers, depicted in Fig. 4: *Data Layer*, *Logic Layer* and *Visualisation Layer*. The *Backend* and *Frontend* layers are used only as meta-layers for our proof-of-concept implementation of the MyAQI. The data layer retrieves the data

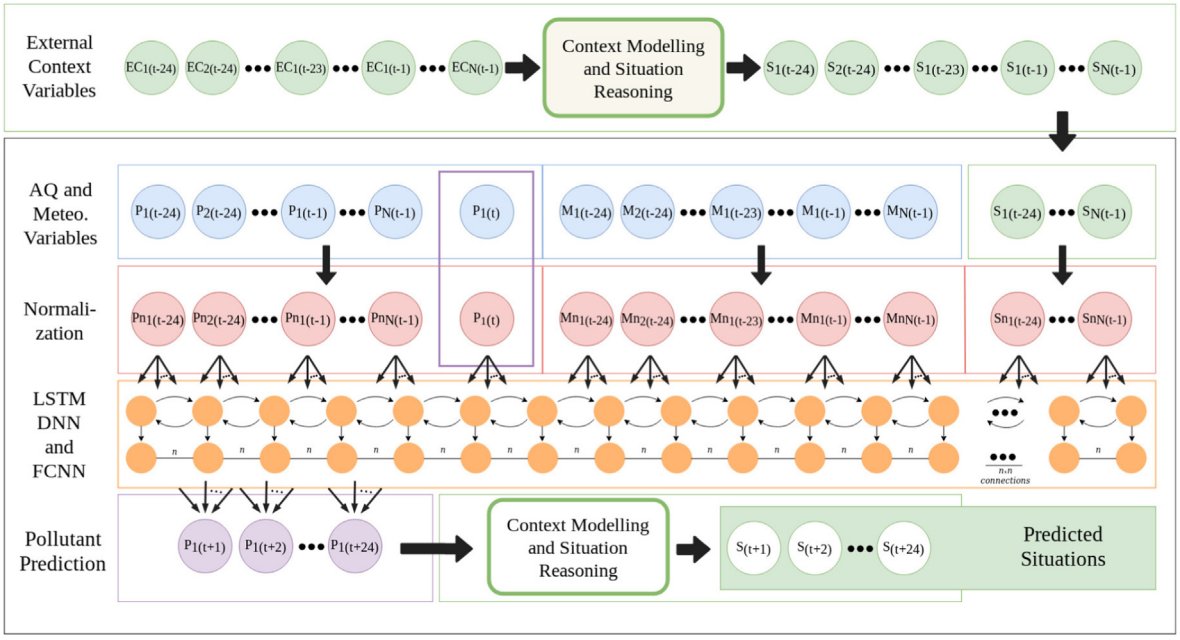

Fig. 3. The MyAQI system prediction model structure and general prediction work-flow.

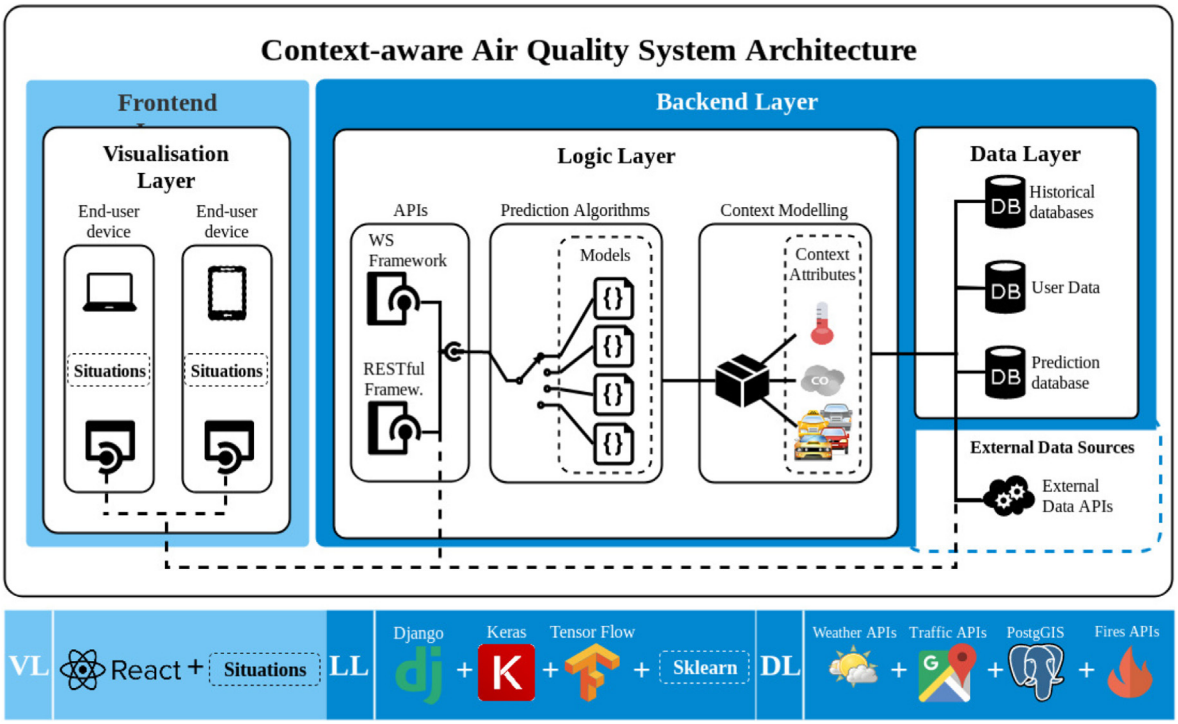

Fig. 4. MyAQI system layers and overall architecture.

required to fuel the context model attributes from external api for the AQ, fire incidents and traffic volumes data, and data stored in relational databases, along with user-entered information. The logic layer is comprised by three modules: (i) the context modelling module, that maps the raw data into usable context attributes, (ii) the prediction algorithm module which executes data analysis, such as prediction, on the context attributes, to augment the known information, and (iii) the MyAQI.

API module which has two interfaces, a restful htt p api for regular exchange of information with the frontend modules and a ws interface for push notification from the backend server to the user devices. Finally, the frontend layer has only one sub-layer, in charge of the context-aware visualisation of AQ data. The modules of the *Visualisation Layer* are: (i) api consumer, which maps incoming sever information into memory objects, which are then passed to the (ii) *Situation Reasoning* module, where the context states are mapped into real-life events, which are then visualised in the (iii) end-user device views.

Fig. 4 also presents some of the technologies and frameworks used in the prototype implementation of the MyAQI system. *PostGIS* is used for geographical queries, needed for the distance from users to fires incidents, for example. Reasoning functionalities, such as prediction, are implemented with the *Python* machine learning framework *Keras* (with a *TensorFlow* backend). Finally, the api modules are implemented using *Django Rest Framework* for the RESTful API and *Django Channels*, plus the in-memory database *Redis*, for the WebS interface. The frontend layer was built using *ReactJS*.

4. MyAQI – The melbourne use case

A real-life use case set up in the Melbourne Urban area in Victoria (Australia) was conducted to both show the practicability of MyAQI and evaluate its performance. Melbourne has been chosen as it seems to us a favorable environment to test different AQ scenarios. Indeed, the Melbourne region suffers under extensive bushfire incidents on the late summer and early autumn months, which leads to high and sudden increases in airborne pollution levels. The inner city area is also negatively influenced from high levels of pollution due to the increase in traffic during rush hours, mainly on the early morning and late afternoon periods.

In section 4.1, we provide greater details about the Melbourne scenario, especially the data sources used in the context modelling stage. Section 4.3 focuses on evaluating the accuracy of the AQ predictions achieved with MyAQI.

4.1. Scenario & experimental setup

As a first step, data related to all context attributes considered in MyAQI (*cf.*, Table 4) must be collected. In this respect, the following data sources were used as part of the Melbourne use case:

- *Weather & Pollutant station(s):* since urban locations that suffer most from large wildfire are the outskirts of cities, two countryside stations located in *Mooroolbark* and *Traralgon* are selected. Since urban locations suffering from traffic pollution are located close to the city center, two AQ measuring stations are selected, located in *Melbourne CDB* and *Alphington*;
- *Traffic measuring station(s):* for each AQ station, one to four nearby traffic measuring stations where selected to obtain the number of vehicles driving past the site every hour. The *SCATS* system developed by the government of New South Wales is used in this respect, which reports every 15min the number of cars on each major crossing in the city. The *VicRoads* and *Bing Maps* live traffic incidents feeds are also used, as well as the *Google Maps* traffic map layer;
- *Fire measuring station(s):* for the countryside stations (*Traralgon* and *Mooroolbark*), a radius of up to 100 km has been set up to encompass the fires that could affect the pollutant concentration levels at the measuring sites, and up to 20 km inside the city

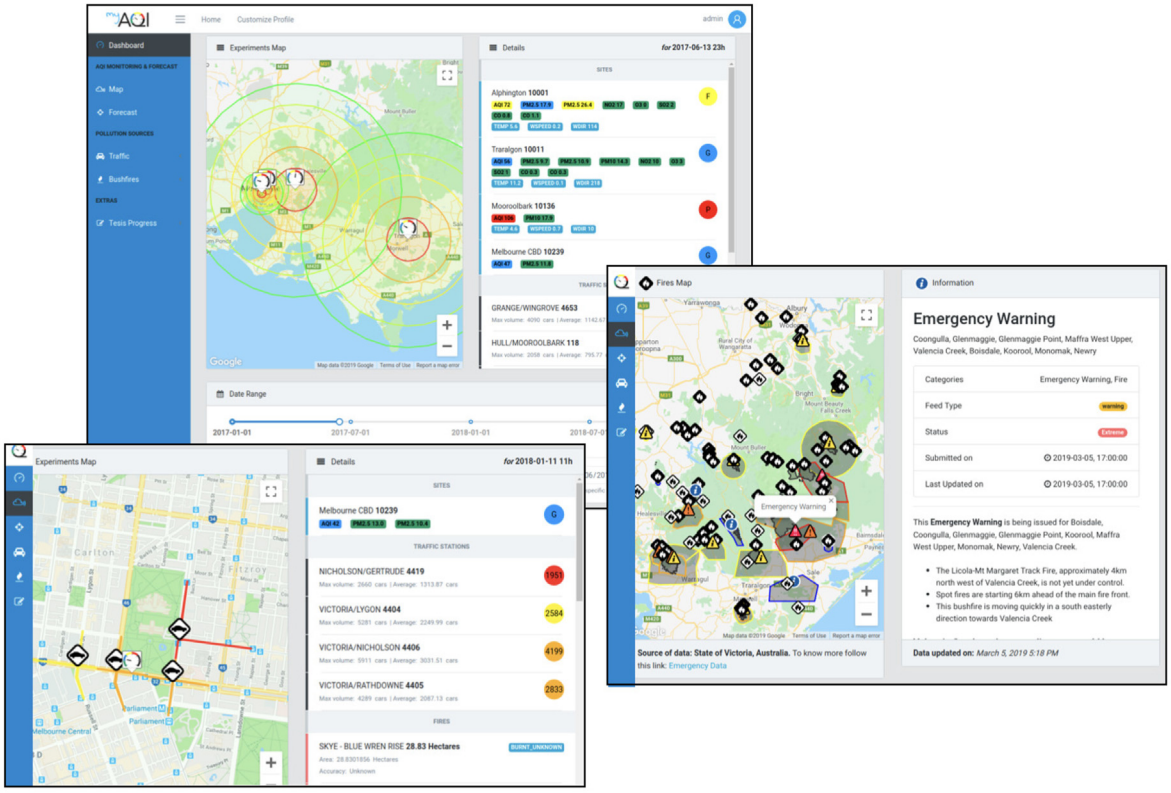

(a) MyAQI UI displaying (i) the four AQ stations; (ii) traffic monitoring stations in *Melbourne CBD*; (iii) live Victoria emergency fires.

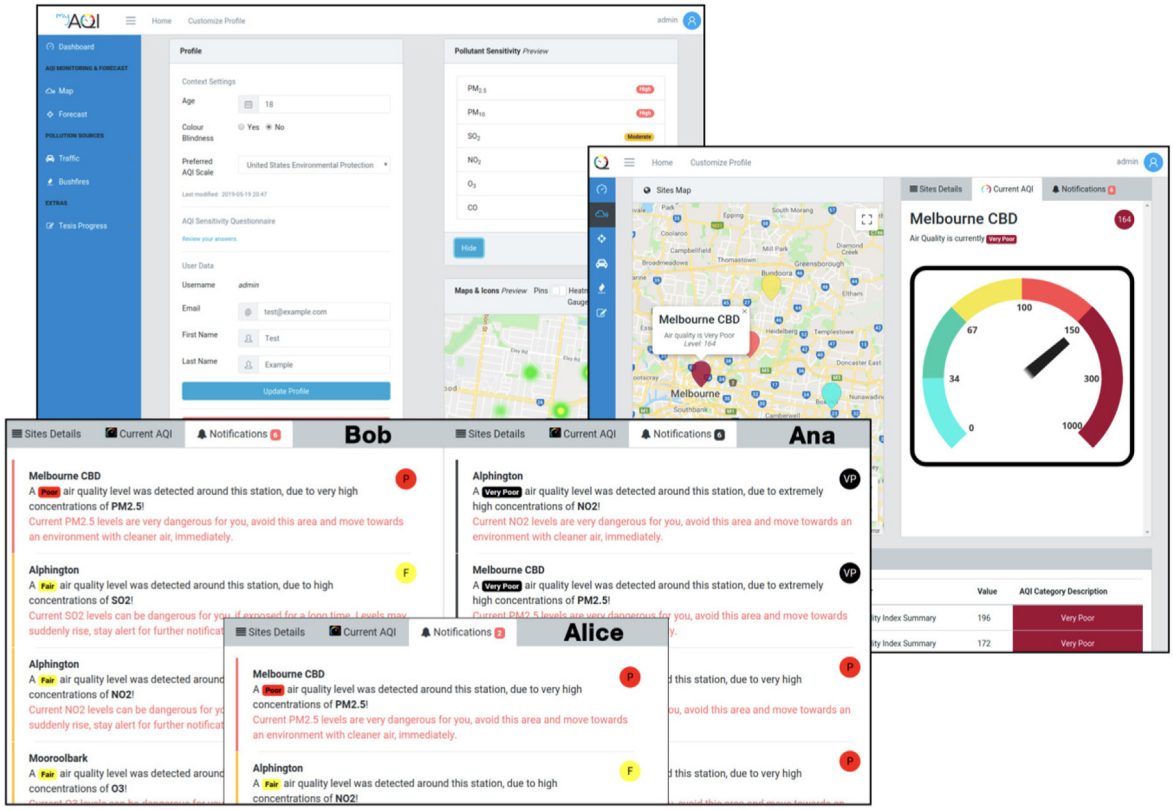

(b) MyAQI UI showing context-aware (i) user profile dashboard; (ii) main AQ monitoring view; (iii) context-aware notifications (see Table 8).

Fig. 5. Web interface screenshots of MyAQI.

limits. To access datasets related to fire incidents (e.g., bushfires, household fires), we use an API of the Victoria government[2] that keeps track of every fire reporting, among other information, the geographical area, starting date, the fire severity (using a four-scale rating system), and so forth. The Victoria Emergency live feed[3] is also considered, providing updated information (every minute) about urgent incidents happening in the region such as fire incidents;

- *Pollutants:* the AirWatch live API[4] maintained by Victoria's AU-EPA branch is used to collect data related to the considered pollutant and meteorological attributes, as detailed in Table 4. This API gathers sensor data streams generated by stations distributed throughout Victoria.

Fig. 5(a) shows three distinct user interface of MyAQI. The first interface (see screenshot denoted by ❶) displays the four AQ stations in our use case, along with the rings of fire situations that would affect them at different severity levels. The second one (see screenshot ❷) shows the traffic monitoring stations surrounding the *Melbourne CBD*'s AQ station, and the influence of traffic volumes on pollution levels. The third one (see screenshot ❸) displays the locations of the different fire incidents raised by the Victoria's emergency system.

In Fig. 5(b), three additional user interfaces are given, showing how MyAQI deals with context-aware user profile for personalisation. The first interface (see screenshot ❹) presents the user profile page on which users can specify their own attributes (e.g., by answering health status questions) and preferences (e.g., preferred AQI scale). The second interface (see screenshot ❺) is the AQI page, which provides each user with the computed personalised AQI (e.g., the eea AQI scale was preferred in this example). The last interface (see screenshot ❻) corresponds to the notification webpage where users are alerted when they are in critical situations from an air quality viewpoint. The scenario depicted through interface ❻ is interesting as it shows that, for three different user profiles: Alice, Bob, Ana (each profile being described in Table 8), they all receive different alerts for a same pollutant level; Ana, for example, has the most delicate health condition because of her asthma, and consequently receives more severe alerts than Bob and Alice.

4.2. Data analysis

It is important to understand the possible correlation between the different context attributes in order to know when to include each attribute during the prediction of one of the pollutants. The data analysis allows us to acknowledge this relationships and to grasp the implications from one attribute to another. When predicting future concentration levels of pollutants, the more attributes that truly explain their behaviour we include, the more accurate the prediction will be.

Fig. 6 provides insight into the context attribute values (time-series) related to the four the AQ stations for a short period of time. This allows to better understand the behaviour of the variables and see their relation at specific points in time. For the two stations located in the outskirts of the Melbourne urban area, Mooroolbark and Traralgon, the fire activity is significant during the period between February and May and have influence on some high peaks of $PM_{2.5}$ and pm_{10} levels, obviously rising the AQI levels as well. For the city-located stations, Melbourne CBD and Alphington, the traffic levels influence in the fluctuation of pollutants such as $PM_{2.5}$ and O_3, specially on rush-hour traffic time ranges, roughly from 7am to 9am and 5pm−7pm, as well as before or during some events and holidays such as new years eve for example. Furthermore, the context of such events could be added to the prediction to know when to expect high traffic volumes due to the creation of an event in a close-by location.

Another insightful analysis is obtained through correlation heatmaps, as presented in Fig. 7. We can conclude again, that in the city fire has no incidence over aqi levels, but traffic does, and the other way around on the countryside. Furthermore, some pollutants are strongly related, like $PM_{2.5}$ and CO levels, as stated throughout the literature as well. Important to notice is that the pollutants that mostly affect AQI levels are$PM_{2.5}$, PM_{10} and NO_2, being these also the most hazardous ones. And finally we notice that the biggest connection between pollutants and meteorological factors is that of O_3 and temperature, because on days with higher temperatures, NO_2 molecules "attack" oxygen molecules, by freeing an oxygen atom and generating ozone.

Table 8
Example of three user profiles w.r.t health and pollutants.

User	Health Condition	Pollutant sensitivity
Alice	Completely healthy	0 - Neutral
Bob	Unhealthy diet, casual smoker…	2 - Moderate
Ana	Has asthma	4 - Extremely High

4.3. Prediction results

Performance of the prediction algorithm underlying the MyAQI system has been evaluated, by comparing the prediction results with the ground truth (i.e., real AQ values). Note that our experiments were conducted based on context attribute record values collected from Jan. 2017 to Jan. 2019.

Ground truth-based evaluation: Fig. 8(a) and (b) present the prediction performance of stations located inside the city centre in Melbourne. The former frame shows the values for a 1-h-ahead prediction of $PM_{2.5}$ levels made on the Melbourne CBD station, using only values for the previous 24 h on $PM_{2.5}$ concentrations and the traffic volume information for four of the traffic measuring stations, presenting a good performance. Frame (b) on the same figure, shows the values for a 1-h-ahead prediction of $PM_{2.5}$ concentrations in the Alphington AQ measuring station using NO_2, SO_2, PM_{10} and CO, besides the traffic volume information for the closest traffic station to the AQ measuring station; the outcome of this prediction is much more accurate given the higher availability of data. The previous two results show the benefits of using traffic information for predicting $PM_{2.5}$ values. And for the rest of the AQ stations, which are located in a more rural area, the prediction is augmented by the use of fire incident information. In Fig. 8(c) and (d) present the $PM_{2.5}$ predictions on the Mooroolbark and Traralgon stations respectively. The first one uses historical $PM_{2.5}$ and PM_{10} concentrations added to fire incidents to forecast future $PM_{2.5}$ levels; when pollution rises abruptly, the prediction takes a bit to adapt, but it quickly follows the ground truth. For the latter station, the prediction shows a close to real-situation performance. All four pictures present coloured backgrounds, that represent the AQ situations for $PM_{2.5}$ concentration levels, this shows the precision of the prediction to be quite high, as most of the predicted situations fall within the real ones. Furthermore, Table 9 shows the comparison of predictions' MAE, RMSE, precision and correlation (R) values for the four stations, once with extended context and once without

[2] https://discover.data.vic.gov.au/dataset/fire-history-records-of-fires-primarily-on-public-land, last access Aug. 2019.
[3] https://www.emergency.vic.gov.au/, last access Aug. 2019.
[4] http://sciwebsvc.epa.vic.gov.au/aqapi/, last access Aug. 2019.

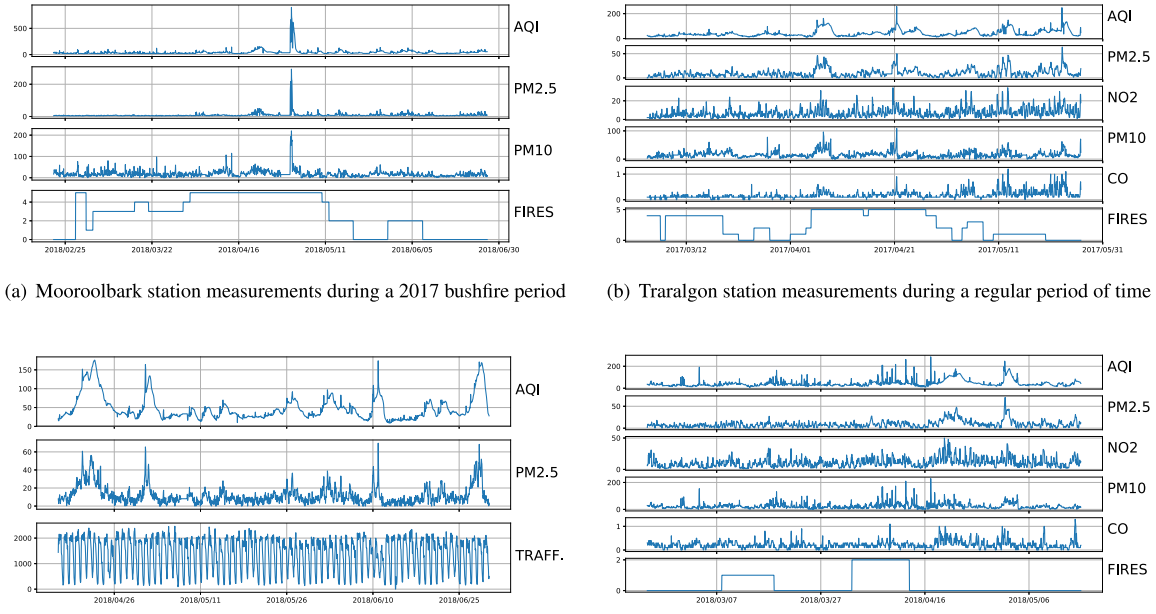

(a) Mooroolbark station measurements during a 2017 bushfire period

(b) Traralgon station measurements during a regular period of time

(c) Melbourne CBD station measurements during a 2017 bushfire period

(d) Alphington station measurements during a regular period of time

Fig. 6. Snapshots of context attributes' time-series for each AQ monitoring station.

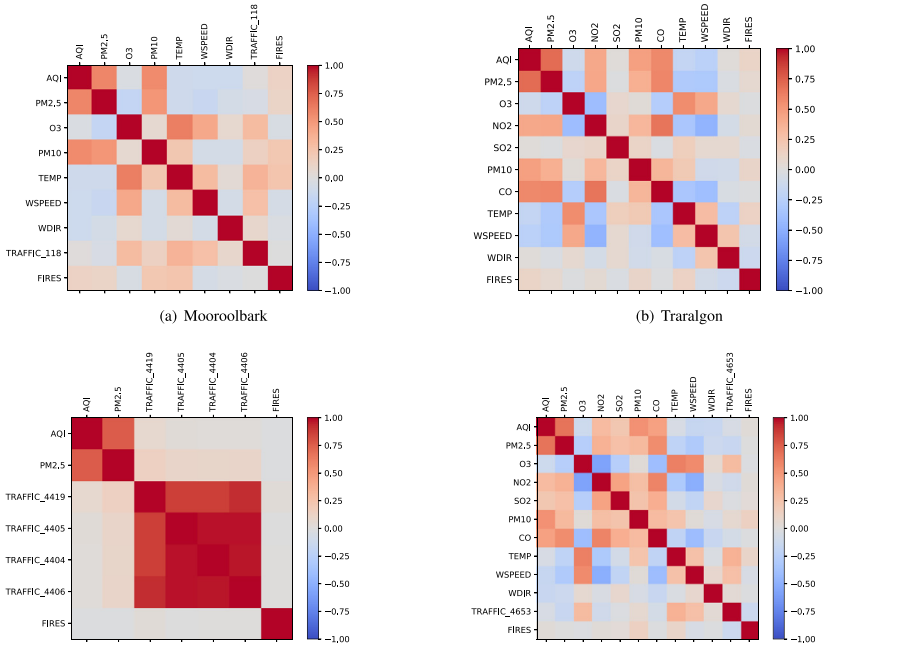

(a) Mooroolbark

(b) Traralgon

(c) Melbourne CBD

(d) Alphington station measurements during a regular period of time

Fig. 7. Correlation heatmap analysis of context attributes for each AQ monitoring station.

against the ground truth. For all stations, except Alphington, the improvement in prediction is clear when using the extended environmental context. The case with Alphington can be interpreted as a lack of correlation between extended context variables and the AQ in the area, probably coming from another pollution source. Precision, which measures the accuracy of the classification of situations after the forecast, is always improved in the other three stations, specially in Mooroolbark and Traralgon, which are influenced the most by bushfires.

5. Conclusion, implications, limitations & future research

5.1. Conclusions

Providing accurate and customised air quality predictions to city stakeholders is a critical task, due to the life threatening hazards that high air pollution levels can pose to humans. Aiming at extending previous research, which mostly focuses on improving the underlying algorithms themselves, we include context-aware computing to the prediction model. The goal is to personalise the

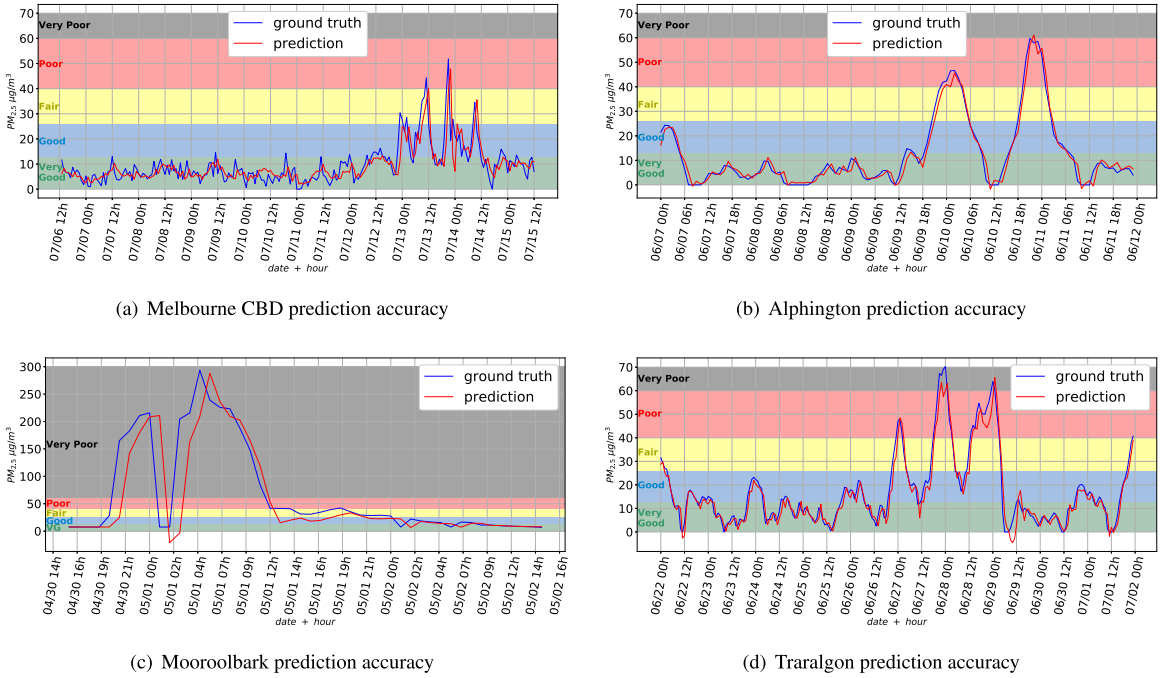

(a) Melbourne CBD prediction accuracy

(b) Alphington prediction accuracy

(c) Mooroolbark prediction accuracy

(d) Traralgon prediction accuracy

Fig. 8. Prediction precision comparison for the four AQ monitoring stations time-series.

Table 9
Comparison of MAE, RMSE, precision and R values for the prediction results from the LSTM model with and without extended context values, for all four AQ stations.

		Performance Indicators			
Station	Attributes	MAE	RMSE	Precision	R
Traralgon AQ station	+1hr *PM2.5 prediction*				
Without Extended Context	PM2.5, PM10, NO2, SO2, CO	1.678	2.411	0.916	0.776
With Extended Context	+ Fires	1.477	2.262	0.943	0.772
Mooroolbark AQ station	+1hr *PM2.5 prediction*				
Without Extended Context	PM2.5, PM10	4.295	6.769	0.872	0.583
With Extended Context	+ Traffic, Fires	2.124	8.775	0.909	0.629
Alphington AQ station	+1hr *PM2.5 prediction*				
Without Extended Context	PM2.5, pm10, no2, so2, co	1.364	1.922	0.956	0.788
With Extended Context	+ Traffic, Fires	1.389	1.949	0.957	0.791
Melbourne CBD AQ *station*	+1hr *PM2.5 prediction*				
Without Extended Context	PM2.5	2.869	4.115	0.912	0.233
With Extended Context	+ Traffic	2.797	3.85	0.93	0.353

output and improve the prediction precision by considering nearby pollution sources. In this respect, we present a novel context- and situation model for AQ monitoring and prediction, which is called MyAQI (standing for "My Air Quality Index"). The well-known LSTM DNN is used as underlying prediction technique, combined with airborne-pollution data sources that have never been considered in the literature to the best of our knowledge. MyAQI was applied in the Melbourne Urban Area (Victoria, Australia), showing that the prediction accuracy is increased up to 3% for some of the monitoring stations.

Furthermore, by capitalising on the benefits of context-aware computing, we are able to tailor the prediction and monitoring outputs depending on the health conditions of each individual user (i.e., depending on individual sensitivities to airborne pollution). This is rarely seen across related work and is critical for the understanding of the AQ problem faced in cities.

5.2. Implications

This research presents two main theoretical implications.

First, it has implications in the field of AQ prediction, where it explores the possibility of adding pollution sources directly to the prediction model. There is previous research that considers only context information for the prediction process (Catalano and Galatioto, 2017) and others that purely enhance the latest prediction algorithms considering only feature extraction from the air pollutant concentrations and meteorological factors time-series (Qi et al., 2019; Wen et al., 2019; Zhou et al., 2019). Given the localised nature of AQ we look for a balance, that considers long term time-series and short-term pollution sources that could create low-frequency high peaks of pollution, which is extremely hard to predict; without neglecting the need for a robust machine learning prediction algorithm. Our results motivate further exploration of combining these approaches.

Second, the proposed approach also contributes to the increasing professional and public awareness of how AQ affect cities and citizens, thus enabling better decisions to be made for the public health and city planning sectors. Our customisation results raise the awareness of the individual citizen and how air pollution might affect them, unfolding a large number of chain effects.

Following a sustainability impact framework for ICT solutions presented in (Duboc et al., 2019), the influence and benefit of this research work can be declined into five sectorial areas, namely: *(i-iii) economic, technical & environmental:* due to transparency and consciousness of the community, the mitigation of their emissions will take more importance over economic growth during important decisions, enabling the further creation of new and better environmental monitoring tools; *(iv-v) individual and social:* citizens and communities understand the AQ problem and avoid polluted areas, participate in regulation changes and demand more environmentally aware governments, producing reports as shown in (Zhou et al., 2018).

5.3. Limitations & future research

Several limitations of our work can be raised. First, the usage of real-life data sources introduces uncertainties because of potential disturbances or malfunctioning of the measuring stations, which is important aspect to tackle (Saylor et al., 2019). With better and more reliable mobile data sources (e.g., by fitting each user with individual air pollution devices, algorithms such as the one presented in (Mihăiţă et al., 2019) or discussed in (Saylor et al., 2019) could be explored.

Second, pollution sources considered in this work (e.g., traffic and fire incidents) are only two members of a large group, which includes factories, air planes, but also extreme natural phenomena such as volcanic eruptions. Such pollution sources should be taken into account in future research.

Third, it is challenging to compare our approach with state-of-the-art studies due to the fact that, to the best of our knowledge, no study has ever considered fire and traffic monitoring stations in context-aware AQ models. Having said that, our study could be used as benchmark for future studies proposing context-aware AQ models.

CRediT authorship contribution statement

Daniel Schürholz: Conceptualization, Methodology, Software, Writing - original draft. **Sylvain Kubler:** Supervision, Writing - review & editing. **Arkady Zaslavsky:** Supervision, Writing - review & editing, Project administration.

Declaration of competing interest

The authors declare that they have no known competing financial interests or personal relationships that could have appeared to influence the work reported in this paper.

Acknowledgments

The research reported here was supported and funded by the PERCCOM Erasmus Mundus Program of the European Union (PERCCOM- FPA 2013-0231). The authors would like to express their gratitude to all the partner institutions, sponsors, and researchers involved in the PERCCOM program (Klimova et al., 2016). Part of this work has been carried out in the scope of the project bIoTope which is co-funded by the European Commission under the Horizon-2020 program, contract number H2020-ICT-2015/688203 – bIoTope.

Appendix A. Abbreviations & Units

$\mu g/m^3$	micro grams per cubic meter
°C	degree Celsius
m/s	meters per second
AE	Auto-Encoders
Af	Accuracy factor
ANN	Artificial Neural Networks
API	Application Programming Interface
AQ	Air Quality
AQI	Air Quality Index
ARE	Average Relative Error
ARIMA	Autoregressive Integrated Moving Average
ARMA	Autoregressive Moving Average
AU-EPA	Australian Environmental Protection Agency
BP	Back-Propagation Algorithm
BPNN	Back-Propagation Neural Network
C-LSTME	Extended Convolutional Long-short Term Memory Neural Network
CEEMD	Complementary Ensemble Empirical Mode Decomposition
CL	Cloudiness
CNN	Deep Convolutional Networks
CO	Carbon Monoxide
CO2	Carbon Dioxide
CSA	Cuckoo's Search Algorithm
DM-LSTM	Deep learning-based Multi-output LSTM
DNN	Deep Learning Neural Network
DP	Dew Point
DR	Detection Rate
DT	Decision Tree
DynPT	Dynamic Pre-Training
EEA	European Environmental Agency
EEMD	Ensemble Empirical Mode Decomposition
Ef	Coe_cient E_ciency
FAC2	Fraction Values within a factor of 2
FAR	False Alarm Rate
FB	Fractional Bias
FF	Feed Forward Algorithm
FFA	Ford–Fulkerson Algorithm
GA	Genetic Algorithm
Gbench	Goodness-to-fit with respect to benchmark
GCA	Gray Correlation Analysis
GCN	Graph Convolutional Network
GFM-NN	Geographic Forecasting Models with Neural Networks
GRNN	Generalized Regression Neural Network
GRU	Gated Recurrent Unit
GT	Geographic Trajectories
HC	Hydrocarbon
HMM	Hidden Markov Models
HSMM	Hidden Semi Markov Models
HTTP	Hyper Text Transfer Protocol
IA	Index of Agreement
K–S	Kolmogorov–Smirnov test
L	Luminosity
LM	Levenberge-Marquardt
LR	Linear Regression
LS-SVM	Least Square Support Vector Machines
LSTM	Long Short-Term Memory Neural Network
MA	Moving Average
MAD	Median Absolute Deviation
MAE	Mean Absolute Error
MAPE	Mean Absolute Percentage Error
MLP	Multi-Layer Perceptron
MLR	Multi Linear Regression
MP5	Multivariate Regression Tree
MPR	Multivariate Polynomial Regression
MSE	Mean Square Error
MyAQI	My Air Quality Index
NMSE	Normalised Mean Square Error

NO	Nitrogen Monoxide
NO_2	Nitrogen Dioxide
NOx	Nitrogen Monoxide/Dioxide
NPEt	Normalised Percent Error
O_3	Ozone
OWA	Ordered Weighted Averaging
P	Precipitation
PA	Prediction Accuracy
PCA	Principal Component Analysis
PDF	Probability Distribution Function
PEt	Percent Error
PLSR	Partial Least Squares Regression
PM	Particle Matter
PM_{10}	Particle Matter under 10 _ m of diameter
$PM_{2.5}$	Particle Matter under 2.5 _ m of diameter
ppb	parts per billion
ppm	parts per million
PSOGSA	Particle Swarm Optimization and Gravitational Search Algorithm
PTA	Prediction Trend Accuracy
R	Correlation Coe_cient
RBFNN	Radial-Basis Function Neural Network
RBM	Restricted Boltzmann Machine
RESTful	Representational State Transfer
RF	Random Forest
RH	Relative Humidity
RMSE	Root Mean Square Error
RNN	Recurrent Neural Network
RP	Relative Pressure
RR	Average Recall Rate
RT	Regression Tree
SARIMA	Seasonal Autoregressive Integrated Moving Average
SEP	Standard Error of Perception
SI	Success Index
SM-LSTM	Shallow Multi-output LSTM Neural Network
SO_2	Sulphur Dioxide
SR	Solar Radiation
STDL	Spatio-Temporal Deep Learning model
SVM	Support Vector Machines
SVR	Support Vector Regressor
T	Temperature
TLNN	Time Lagged Neural Networks
TPR	True Prediction Rate
US-EPA	United States Environmental Protection Agency
V	Visibility
WavD	Wavelet Decomposition
WD	Wind Direction
WebS	Web Sockets
WS	Wind Speed

Appendix B. Air Quality Indexes

Tables B10, B11 and B.12 present the aqis for the US-EPA, EEA and AU-EPA, respectively. In each table the pollutant concentrations are mapped to the respective AQI values, colours and descriptions.

Table B.10
Mapping pollutants concentrations to the US-EPA AQI values and categories.

This category…	… equals this AQI	… and these Breakpoints						
	AQI	O_3 (ppm) 8-h	O_3 (ppm) 1-h	$PM_{2.5}$ ($\mu g{=}m^3$) 24-h	PM_{10} ($\mu g{=}m^3$) 8-h	CO (ppm) 8-h	SO_2 (ppb) 1-h	NO_2 (ppb) 1-h
Good	0–50	0.000–0.054	–	0.0–12.0	0–54	0.0–4.4	0–35	0–53
Moderate	51–100	0.055–0.070	–	12.1–35.4	55–154	4.5–9.4	36–75	54–100
Unhealthy for Sensitive Groups	101–150	0.071–0.085	0.125–0.164	35.5–55.4	155–254	9.5–12.4	76–185	101–360
Unhealthy	151–200	0.086–0.105	0.165–0.204	55.5–150.4	255–354	12.5–15.4	186–304	361–649
Very unhealthy	201–300	0.106–0.200	0.205–0.404	150.5–250.4	355–424	15.5–30.4	305–604	650–1249
Hazardous	301–400	–	0.405–0.504	250.5–350.4	425–504	30.5–40.4	605–804	1250–1649
Hazardous	401–500	–	0.505–0.604	350.5–500.4	505–604	40.5–50.4	805–1004	1650–2049

Table B.11
Mapping pollutants concentrations to the EEA AQI categories.

Band Descriptor	O_3	NO_2	PM_{10}	$PM_{2.5}$	SO_2
	1-h ($\mu g{=}m^3$)	1-h ($\mu g{=}m^3$)	Running 24-h ($\mu g{=}m^3$)	Running 24-h ($\mu g{=}m^3$)	1-h ($\mu g{=}m^3$)
Good	0–80	0–40	0–20	0–10	0–100
Fair	81–120	41–100	21–35	11–20	101–200
Moderate	121–180	101–200	36–50	21–25	201–350
Poor	181–240	201–400	51–100	26–50	351–500
Very Poor	>240	>400	>100	>50	>500

Table B.12
Mapping pollutants concentrations to the AU-EPA AQI categories.

Pollutant	$PM_{2.5}$ (24-h) ($\mu g{=}m^3$)	$PM_{2.5}$ (1-h) ($\mu g{=}m^3$)	PM_{10} (1-h) ($\mu g{=}m^3$)	CO (1- hour) ppm	SO_2 (1- hour) ppb	NO_2 (1- hour) ppb	O_3 (1- hour) ppb	V (1-h)
Very Good	0–8.2	0–13.1	0–26.3	0–2.9	0–65	0–39	0–33	0–0.77
Good	8.3–16.4	13.2–26.3	26.4–52.7	3.0–5.8	66–131	40–78	34–66	0.78–1.56
Moderate	16.5–24.9	26.4–39.9	52.8–79.9	5.9–8.9	132–199	79–119	67–99	1.57–2.34
Poor	25.0–37.4	40–59.9	80–119.9	9.0–13.4	200–299	120–179	100–149	2.35–3.52
Very Poor	37.5 or greater	60 or greater	120 or greater	13.5 or greater	300 or greater	180 or greater	150 or greater	3.53 or greater

Appendix C. AQ Situations for the US-EPA and EEA AQIs

Table C13 describes the AQ situations for different user pollutant sensitivities when considering the USEPA and EEA AQI, respectively.

Table C.13
Situation spaces definitions for US-EPA and EEA AQIs in relation to the user's pollutant sensitivities.

EEA AQI categories	User Sensitivity Levels				
	0	1	2	3	4
Good	0 - 33	0 - 33	0 - 33	0 - 33	0 - 23
Fair	34 - 66	34 - 66	34 - 66	34 - 54	24 - 44
Moderate	67 - 99	67 - 99	55 - 79	55 - 79	45 - 59
Poor	100 - 149	100 - 124	80 - 99	80 - 89	60 - 69
Very Poor	150 or greater	125 or greater	100 or greater	90 or greater	70 or greater
US-EPA AQI categories	0	1	2	3	4
Good	0 - 50	0 - 50	0 - 50	0 - 50	0 - 33
Moderate	51 - 100	51 - 100	51 - 100	51 - 80	34 - 60
Unhealthy for Sensitive Groups	101 - 150	101 - 150	101 - 130	81 - 100	61 - 85
Unhealthy	151 - 200	151 - 190	131 - 150	101 - 115	86 - 105
Very unhealthy	201 - 300	191 - 230	151 - 165	116 - 130	106 - 115
Hazardous	301 or greater	231 or greater	166 or greater	131 or greater	116 or greater

Appendix D. LSTM Neural Network

The main improvement of LSTMs takes place in the memory blocks. Each block is composed by various memory cells (which in turn can be connected to itself) and by multiplicative gates. The gates are for input, output and forgetting tasks. These tasks can be mapped to read, write and reset operations, respectively. The input gate controls if the cell's internal state is to be affected by incoming signals and the output gate controls if the result of the cell's processing will affect other cells. But the novel concept in a LSTM neuron structure is the forget gate, which resets the cells state once the information held by it is outdated thus preventing the saturation of the squashing function, that occurs with the out-of-bounds growth of a cell's state. The state itself is maintained by the activation of a self-connected linear unit-constant error carousel (CEC), which is part of the cells memory and can stop any stimulus coming from the outside, thus retaining the same state over certain periods of time. This feature allows LSTMs to solve the vanishing gradient problem, that is accentuated with the increase of layers with different activation functions making the gradient of the loss function approach zero, affecting the networks ability to train.

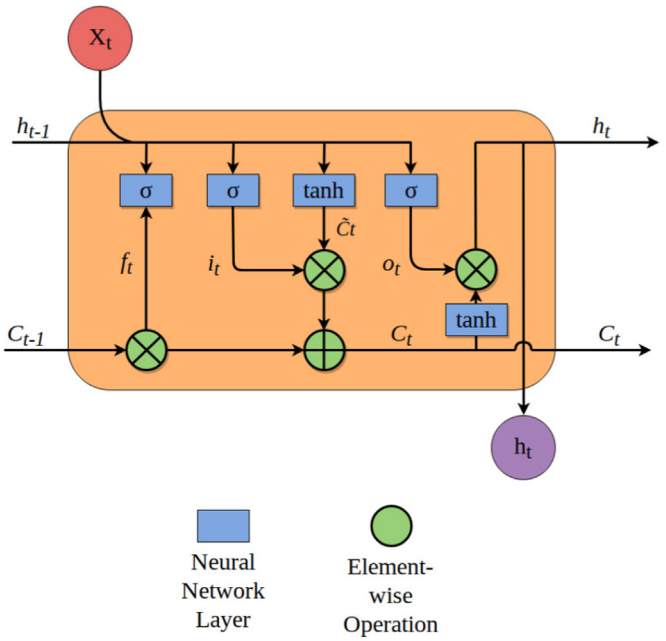

Figure D.9. A L memory block with one memory cell.

The input of the block is represented by X_t where $X = (X_1, X_2 \ldots, X_N)$ and $X_i \in R^T$; N is the number of dimensions in the input, T the time lag and $Y = (Y_1, Y_2 \ldots, Y_N)$ the output values. For the MyAQI system's AQ prediction use case, X vectors take the values of the AQ, meteorological and extended context attributes; the Y vector takes the values of the desired to-be-predicted pollutant's predicted concentrations. The functions denoted in Figure D9 by the free floating letters are characterised by the following equations:

$$f_t = \sigma\left(W_f \cdot [h_{t-1}, X_t] + b_f\right) \tag{D.1}$$

$$i_t = \sigma(W_i \cdot [h_{t-1}, X_t] + b_i) \tag{D.2}$$

$$C_t = f_t * C_{t-1} + i_t * tanh(W_C \cdot [h_{t-1}, X_t] + b_C) \tag{D.3}$$

$$o_t = \sigma(W_o \cdot [h_{t-1}, X_t] + b_o) \tag{D.4}$$

$$h_t = o_t * tanh(C_t) \tag{D.5}$$

where f_t denotes the forget gate, i_t the input gate and o_t the output gate. $\sigma(\cdot)$ stands for the sigmoid function and $tanh(\cdot)$ the tanh function, defined in function D.6 and D.7, respectively. C_t and h_t are the activation vector for each cell and memory block, respectively. W represents the weight matrix and b the bias vector.

$$\sigma(x) = \frac{1}{1 + e^{-x}} \tag{D.6}$$

$$tanh(x) = \frac{e^x - e^{-x}}{e^x + e^{-x}} \tag{D.7}$$

References

Air index EEA map. http://airindex.eea.europa.eu/. (Accessed 13 April 2020).

Athira, V., Geetha, P., Vinayakumar, R., Soman, K.P., 2018. Deepairnet: applying recurrent networks for air quality prediction. Procedia computer science 132, 1394–1403.

Australian Government, National Clean Air Agreement, 2018. Technical Report. http://www.environment.gov.au/protection/air-quality/national-clean-air-agreement. (Accessed 13 April 2020).

Bai, Y., Li, Y., Wang, X., Xie, J., Li, C., 2016. Air pollutants concentrations forecasting using back propagation neural network based on wavelet decomposition with meteorological conditions. Atmospheric pollution research 7 (3), 557–566.

Becerra, J.A., Lizana, J., Gil, M., Barrios-Padura, A., Blondeau, P., Chacartegui, R., 2020. Identification of potential indoor air pollutants in schools. J. Clean. Prod. 242, 118420.

Biancofiore, F., Busilacchio, M., Verdecchia, M., Tomassetti, B., Aruffo, E., Bianco, S., Di Tommaso, S., Colangeli, C., Rosatelli, G., Di Carlo, P., 2017. Recursive neural network model for analysis and forecast of PM10 and PM2. 5. Atmospheric Pollution Research 8 (4), 652–659.

Catalano, M., Galatioto, F., 2017. Enhanced transport-related air pollution prediction through a novel metamodel approach. Transport. Res. Transport Environ. 55, 262–276.

Chen, L., Cai, Y., Ding, Y., Lv, M., Yuan, C., Chen, G., 2016. Spatially fine-grained urban air quality estimation using ensemble semi-supervised learning and pruning. In: 2016 ACM International Joint Conference on Pervasive and Ubiquitous Computing (UbiComp), pp. 1076–1087. Heidelberg, Germany, September 12-16.

Cohen, A.J., Brauer, M., Burnett, R., Anderson, H.R., Frostad, J., Balakrishnan, K., Dandona, L., Feigin, V., Hubbell, B., Hubbell, K., Liu, Y., Morawska, L., Shin, H., Shaddick, G., van Dingenen, R., Vos, T., Forouzanfar, M.H., 2017. Estimates and 25-year trends of the global burden of disease attributable to ambient air pollution: an analysis of data from the Global Burden of Diseases Study 2015. Lancet 389 (10082), 1907–1918.

Dean, A., Green, D., 2017. Climate Change, Air Pollution and Health in Australia. UNSW Sydney, Sydney, Australia.

Dhinesh, B., Annamalai, M., 2018. A study on performance, combustion and emission behaviour of diesel engine powered by novel nano nerium oleander biofuel. J. Clean. Prod. 196, 74–83.

Domańska, D., Wojtylak, M., 2012. Application of fuzzy time series models for forecasting pollution concentrations. Expert Syst. Appl. 39 (9), 7673–7679.

Dong, M., Yang, D., Kuang, Y., He, D., Erdal, S., Kenski, D., 2009. PM2.5 concentration prediction using hidden semi-Markov model-based times series data mining. Expert Syst. Appl. 36 (5), 9046–9055.

Donnelly, A., Misstear, B., Broderick, B., 2015. Real time air quality forecasting using integrated parametric and non-parametric regression techniques. Atmos. Environ. 103, 53–65.

Duboc, L., Betz, S., Penzenstadler, B., Kocak, S.A., Chitchyan, R., Leifler, O., Porras, J., Seyff, N., Venters, C.C., 2019. Do we really know what we are building? Raising awareness of potential Sustainability Effects of Software Systems in Requirements Engineering. In: 27th IEEE International Requirements Engineering Conference (RE), pp. 6–16. Jejudo, South Korea, September 23-27.

Dutta, P., Aoki, P.M., Kumar, N., Mainwaring, A., Myers, C., Willett, W., Woodruff, A., 2009. Common sense: participatory urban sensing using a network of handheld air quality monitors. In: 7th ACM Conference on Embedded Networked Sensor Systems (SenSys), pp. 349–350. Berkeley, United States, November 2009.

European Environmental Agency (Eea), 2019. Air quality in Europe – 2019 report. https://www.eea.europa.eu/publications/air-quality-in-europe-2019. (Accessed 13 April 2020).

Ercilla-Montserrat, M., Muñoz, P., Montero, J.I., Gabarrell, X., Rieradevall, J., 2018. A study on air quality and heavy metals content of urban food produced in a Mediterranean city (Barcelona). J. Clean. Prod. 195, 385–395.

Feng, X., Li, Q., Zhu, Y., Hou, J., Jin, L., Wang, J., 2015. Artificial neural networks forecasting of PM2. 5 pollution using air mass trajectory based geographic model and wavelet transformation. Atmos. Environ. 107, 118–128.

Fraser, A., Loader, A., Pang, Y., Stewart, R., Xiao, X., Whitehead, C., 2016. Services to develop an EU air quality index, Final Report. Ricardo Energy & Environment. https://ec.europa.eu/environment/air/pdf/Air%20quality%20index_final%20report.pdf. (Accessed 13 April 2020).

Hochreiter, S., Schmidhuber, J., 1997. Long short-term memory. Neural Comput. 9 (8), 1735–1780.

Holgate, S.T., 2017. 'Every breath we take: the lifelong impact of air pollution' – a call for action. Clin. Med. 17 (1), 8–12.

Huang, S.F., Cheng, C.H., 2008. Forecasting the air quality using OWA based time series model. In: 2008 IEEE International Conference on Machine Learning and Cybernetics (ICMLC), vol. 6, pp. 3254–3259. Kunming, China, July 12-15.

Huang, C.J., Kuo, P.H., 2018. A deep CNN-LSTM model for particulate matter (PM2.5) forecasting in smart cities. Sensors 18 (7), 2220.

Kalisa, E., Fadlallah, S., Amani, M., Nahayo, L., Habiyaremye, G., 2018. Temperature and air pollution relationship during heatwaves in Birmingham, UK. Sustainable cities and society 43, 111–120.

Klimova, A., Rondeau, E., Andersson, K., Porras, J., Rybin, A., Zaslavsky, A., 2016. An international Master's program in green ICT as a contribution to sustainable development. J. Clean. Prod. 135, 223–239.

Kurt, A., Oktay, A.B., 2010. Forecasting air pollutant indicator levels with geographic models 3 days in advance using neural networks. Expert Syst. Appl. 37 (12), 7986–7992.

Li, W., Yi, P., 2020. Assessment of city sustainability– Coupling coordinated development among economy, society and environment. J. Clean. Prod. 256, 120453.

Li, X., Peng, L., Yao, X., Cui, S., Hu, Y., You, C., Chi, T., 2017. Long short-term memory neural network for air pollutant concentration predictions: method development and evaluation. Environ. Pollut. 231, 997–1004.

Ma, J., Ding, Y., Cheng, J.C., Jiang, F., Wan, Z., 2019. A temporal-spatial interpolation and extrapolation method based on geographic Long Short-Term Memory neural network for PM2.5. J. Clean. Prod. 237, 117729.

Ma, J., Ding, Y., Cheng, J.C., Jiang, F., Tan, Y., Gan, V.J., Wan, Z., 2020. Identification of high impact factors of air quality on a national scale using big data and machine learning techniques. J. Clean. Prod. 244, 118955.

Mihăiță, A.S., Dupont, L., Chery, O., Camargo, M., Cai, C., 2019. Evaluating air quality by combining stationary, smart mobile pollution monitoring and data-driven modelling. J. Clean. Prod. 221, 398–418.

Nurgazy, M., Zaslavsky, A., Jayaraman, P.P., Kubler, S., Mitra, K., Saguna, S., 2019. CAVisAP: context-aware visualization of outdoor air pollution with IoT platforms. In: International Conference on High Performance Computing and Simulation (HPCS). July 15-19, 2019, Dublin, Ireland.

Ong, B.T., Sugiura, K., Zettsu, K., 2016. Dynamically pre-trained deep recurrent neural networks using environmental monitoring data for predicting PM 2.5. Neural Comput. Appl. 27 (6), 1553–1566.

Ortiz, G., Caravaca, J.A., Garca-de-Prado, A., Boubeta-Puig, J., 2019. Real-time context-aware microservice architecture for predictive analytics and smart decision-making. IEEE Access 7, 183177–183194.

Padovitz, A., Wai Loke, S., Zaslavsky, A., 2010. Towards a theory of context. In: 8th IEEE Annual Conference on Pervasive Computing and Communications (PerCom Workshops), pp. 38–42. Mannheim, Germany, March 29-April 2.

Perera, C., Zaslavsky, A., Christen, P., Georgakopoulos, D., 2013. Context aware computing for the internet of things: a survey. IEEE communications surveys & tutorials 16 (1), 414–454.

Perez, P., Gramsch, E., 2016. Forecasting hourly PM2. 5 in Santiago de Chile with emphasis on night episodes. Atmos. Environ. 124, 22–27.

Qi, Y., Li, Q., Karimian, H., Liu, D., 2019. A hybrid model for spatiotemporal forecasting of PM2. 5 based on graph convolutional neural network and long short-term memory. Sci. Total Environ. 664, 1–10.

Qiu, H., Yu, I.T.S., Wang, X., Tian, L., Tse, L.A., Wong, T.W., 2013. Season and humidity dependence of the effects of air pollution on COPD hospitalizations in Hong Kong. Atmos. Environ. 76, 74–80.

Saylor, R.D., Baker, B.D., Lee, P., Tong, D., Pan, L., Hicks, B.B., 2019. The particle dry deposition component of total deposition from air quality models: right, wrong or uncertain? Tellus B 71 (1), 1550324.

Shaban, K.B., Kadri, A., Rezk, E., 2016. Urban air pollution monitoring system with forecasting models. IEEE Sensor. J. 16 (8), 2598–2606.

Shi, Y., Xu, M., Zhao, R., Fu, H., Wu, T., Cao, N., 2019. Interactive context-aware anomaly detection guided by user feedback. IEEE Transactions on Human-Machine Systems 49 (6), 550–559.

Sigg, S., 2008. Development of a Novel Context Prediction Algorithm and Analysis of Context Prediction Schemes. Kassel university press GmbH.

Sigg, S., Gordon, D., Von Zengen, G., Beigl, M., Haseloff, S., David, K., 2012. Investigation of context prediction accuracy for different context abstraction levels. IEEE Trans. Mobile Comput. 11 (6), 1047–1059.

Singh, K.P., Gupta, S., Kumar, A., Shukla, S.P., 2012. Linear and nonlinear modeling approaches for urban air quality prediction. Sci. Total Environ. 426, 244–255.

Sun, W., Sun, J., 2017. Daily PM2. 5 concentration prediction based on principal component analysis and LSSVM optimized by cuckoo search algorithm. J. Environ. Manag. 188, 144–152.

Sun, W., Zhang, H., Palazoglu, A., Singh, A., Zhang, W., Liu, S., 2013. Prediction of 24-hour-average PM2. 5 concentrations using a hidden Markov model with different emission distributions in Northern California. Sci. Total Environ. 443, 93–103.

United Nations, 2018. The world's cities in 2018 data booklet, economics & social affairs. https://www.un.org/en/events/citiesday/assets/pdf/the_worlds_cities_in_2018_data_booklet.pdf. (Accessed 13 April 2020).

United States Environmental Protection Agency, 2018. Technical assistance document for the reporting of daily air quality-the air quality index (AQI). Publication No. EPA-454/B-18-007. https://www3.epa.gov/airnow/aqi-technical-assistance-document-sept2018.pdf. (Accessed 13 April 2020).

Victoria, E.P.A., 2013. Future Air Quality in Victoria - Final Report Future Air Quality in Victoria-Final Report. Technical Report. Environmental Protection Agency Victoria Australia, Melbourne.

Wang, J., Song, G., 2018. A deep spatial-temporal ensemble model for air quality prediction. Neurocomputing 314, 198–206.

Wang, B., Hong, G., Qin, T., Fan, W.R., Yuan, X.C., 2019. Factors governing the willingness to pay for air pollution treatment: a case study in the Beijing-Tianjin-Hebei region. J. Clean. Prod. 235, 1304–1314.

Wang, S., Gao, S., Li, S., Feng, K., 2020. Strategizing the relation between urbanization and air pollution: Empirical evidence from global countries. J. Clean. Prod. 243, 118615.

Wen, C., Liu, S., Yao, X., Peng, L., Li, X., Hu, Y., Chi, T., 2019. A novel spatiotemporal convolutional long short-term neural network for air pollution prediction. Sci. Total Environ. 654, 1091–1099.

World Bank Group, 1998. Pollution Prevention and Abatement Handbook. Pulp and Paper Mills. https://www.ifc.org/wps/wcm/connect/bfa0c334-a60b-4b7b-b2f9-bd29d0b6ea18/pulp_PPAH.pdf?MOD=AJPERES&CVID=jkD2451. (Accessed

13 April 2020).
Wu, L., Li, N., Yang, Y., 2018. Prediction of air quality indicators for the Beijing-Tianjin-Hebei region. J. Clean. Prod. 196, 682–687.
Yin, P., He, G., Fan, M., Chiu, K.Y., Fan, M., Liu, C., Pan, Y., Mu, Q., Zhou, M., 2017. Particulate air pollution and mortality in 38 of China's largest cities: time series analysis. Bmj 356, j667.
Zhao, H., Zhang, J., Wang, K., Bai, Z., Liu, A., 2010. A GA-ANN model for air quality predicting. In: IEEE 2010 International Computer Symposium (ICS2010), pp. 693–699. Beijing, China, January 5-7.
Zhou, Z., Guo, X., Wu, H., Yu, J., 2018. Evaluating air quality in China based on daily data: application of integer data envelopment analysis. J. Clean. Prod. 198, 304–311.
Zhou, Y., Chang, F.J., Chang, L.C., Kao, I.F., Wang, Y.S., 2019. Explore a deep learning multi-output neural network for regional multi-step-ahead air quality forecasts. J. Clean. Prod. 209, 134–145.
Zhu, S., Lian, X., Wei, L., Che, J., Shen, X., Yang, L., Qiu, X., Liu, X., Gao, W., Ren, X., Li, J., 2018. PM2.5 forecasting using SVR with PSOGSA algorithm based on CEEMD, GRNN and GCA considering meteorological factors. Atmos. Environ. 183, 20–32.